



## Modelled deposition of nitrogen and sulfur in Europe estimated by 14 air quality model-systems: Evaluation, effects of changes in emissions and implications for habitat protection

Marta G. Vivanco<sup>1</sup>, Mark. R. Theobald<sup>1</sup>, Héctor García-Gómez<sup>1</sup>, Juan Luis Garrido<sup>1</sup>, , Marje Prank<sup>2,3</sup>, Wenche Aas<sup>4</sup>, Mario Adani<sup>5</sup>, Ummugulsum Alyuz<sup>6</sup>, Camilla Andersson<sup>7</sup>, Roberto Bellasio<sup>8</sup>, Bertrand Bessagnet<sup>9</sup>, Roberto Bianconi<sup>8</sup>, Johannes Bieser<sup>10</sup>, Jørgen Brandt<sup>11</sup>, Gino Briganti<sup>5</sup>, Andrea Cappelletti<sup>5</sup>, Gabriele Curci<sup>12</sup>, Jesper H. Christensen<sup>11</sup>, Augustin Colette<sup>9</sup>, Florian Couvidat<sup>9</sup>, Kees Cuvelier<sup>13</sup>, Massimo D'Isidoro<sup>5</sup>, Johannes Flemming<sup>14</sup>, Andrea Fraser<sup>15</sup>, Camilla Geels<sup>11</sup>, Kaj M. Hansen<sup>11</sup>, Christian Hogrefe<sup>16</sup>, Ulas Im<sup>11</sup>, Oriol Jorba<sup>17</sup>, Nutthida Kitwiroon<sup>18</sup>, Astrid Manders<sup>19</sup>, Mihaela Mircea<sup>5</sup>, Noelia Otero<sup>20</sup>, Maria-Teresa Pay<sup>17</sup>, Luca Pozzoli<sup>6,21</sup>, Efisio Solazzo<sup>21</sup>, Svetlana Tsyro<sup>22</sup>, Alper Unal<sup>6</sup>, Peter Wind<sup>22,23</sup> and Stefano Galmarini<sup>21</sup>

<sup>1</sup>Environmental Department, CIEMAT, Madrid, 28040, Spain

<sup>2</sup>Finnish Meteorological Institute, Helsinki, FI00560, Finland

<sup>3</sup>Cornell University, Ithaca, NY, 14850, USA

<sup>4</sup>NILU-Norwegian Institute for Air Research, Kjeller, 2007, Norway

<sup>5</sup>ENEA, Italian National Agency for New Technologies, Energy and Sustainable Economic Development (ENEA), Via Martiri di Monte Sole 4, 40129 Bologna, Italy

<sup>6</sup>Eurasia Institute of Earth Sciences, Istanbul Technical University, Turke

<sup>7</sup>SMHI, Swedish Meteorological and Hydrological Institute Norrköping, Norrköping, Sweden

<sup>8</sup>Enviroware srl, Concorezzo, MB, Italy

<sup>9</sup>INERIS, Institut National de l'Environnement Industriel et des Risques, Parc Alata, 60550 Verneuil-en-Halatte, France

<sup>10</sup>Institute of Coastal Research, Chemistry Transport Modelling Group, Helmholtz-Zentrum Geesthacht, Germany

<sup>11</sup>Department of Environmental Science, Aarhus University, Roskilde, DK-4000, Denmark.

<sup>12</sup>Department of Physical and Chemical Sciences, University of L'Aquila, L'Aquila, Italy

<sup>13</sup>Ex European Commission, Joint Research Centre JRC Institute for Environment and Sustainability I-21020 Ispra (Va), Italy

<sup>14</sup>European Centre for Medium-Range Weather Forecasts, Reading, UK

<sup>15</sup>Ricardo Energy & Environment, Gemini Building, Fermi Avenue, Harwell, Oxon, OX11 0QR, UK

<sup>16</sup>Computational Exposure Division, National Exposure Research Laboratory, Office of Research and Development, United States Environmental Protection Agency, Research Triangle Park, NC,

<sup>17</sup>BSC, Barcelona Supercomputing Center, Centro Nacional de Supercomputaci\_ón, Nexus II Building, Jordi Girona, 29, 08034 Barcelona, Spain

<sup>18</sup>Environmental Research Group, Kings' College London, London, UK

<sup>19</sup>Netherlands Organization for Applied Scientific Research (TNO), Utrecht, The Netherlands

<sup>20</sup>IASS, Institute for Advanced Sustainability Studies, Potsdam, Germany

<sup>21</sup>European Commission, Joint Research Centre (JRC, Ispra (VA), Italy

<sup>22</sup>Climate Modelling and Air Pollution Division, Research and Development Department, Norwegian Meteorological Institute (MET Norway), P.O. Box 43, Blindern, N-0313 Oslo, Norway

<sup>23</sup>Faculty of Science and Technology, University of Tromsø, Tromsø, Norway

Correspondence to: Marta G. Vivanco (m.garcia@ciemat.es)



1       **Abstract.** The evaluation and intercomparison of air quality models is key to reducing model errors  
2       and uncertainty. The projects AQMEII3 and EURODELTA-Trends, in the framework of the Task  
3       Force on Hemispheric Transport of Air Pollutants and the Task Force on Measurements and  
4       Modelling, respectively, (both task forces under the UNECE Convention on the Long Range  
5       Transport of Air Pollution, LTRAP) have brought together various regional air quality models, to  
6       analyze their performance in terms of air concentrations and wet deposition, as well as to address  
7       other specific objectives.

8       This paper jointly examines the results from both project communities by inter-comparing and  
9       evaluating the deposition estimates of reduced and oxidized nitrogen (N) and sulfur (S) in Europe  
10      simulated by 14 air quality model-systems for the year 2010. An accurate estimate of deposition is  
11      key to an accurate simulation of atmospheric concentrations. In addition, deposition fluxes are  
12      increasingly being used to estimate ecological impacts. It is, therefore, important to know by how  
13      much model results differ, and how well they agree with observed values, at least when comparison  
14      with observations is possible, such as in the case of wet deposition.

15      This study reveals a large variability between the wet deposition estimates of the models, with some  
16      performing acceptably (according to previously defined criteria) and others underestimating wet  
17      deposition rates. For dry deposition, there are also considerable differences between the model  
18      estimates. An ensemble of the models with the best performance for N wet deposition was made and  
19      used to explore the implications of N deposition in conservation of protected European habitats.  
20      Exceedances of empirical critical loads were calculated for the most common habitats at a resolution  
21      of 100×100 m<sup>2</sup> within the Natura 2000 network, and the habitats with the largest areas showing  
22      exceedances are determined.

23      Moreover, simulations with reduced emissions in selected source areas indicated a fairly linear  
24      relationship between reductions in emissions and changes in deposition rates of N and S. An  
25      approximately 20% reduction in N and S deposition in Europe is found when emissions at a global  
26      scale are reduced by the same amount. European emissions are by far the main contributor to  
27      deposition in Europe, whereas the reduction in deposition due to a decrease of emissions in North  
28      America is very small and confined to the western part of the domain. Reductions in European  
29      emissions led to substantial decreases in the protected habitat areas with critical load exceedances  
30      (halving the exceeded area for certain habitats), whereas no change was found, on average, when  
31      reducing North American emissions, in terms of average values per habitat.

## 32    **1 Introduction**

33    Improvements have been made in reducing ecosystem exposure to excess levels of acidification in past  
34    decades, largely as a result of declining SO<sub>2</sub> emissions. However, in addition to acidification, emissions  
35    of NH<sub>3</sub> and NO<sub>x</sub> have altered the global nitrogen cycle, resulting in excess inputs of nutrient nitrogen into  
36    terrestrial and aquatic ecosystems (Maas & Grennfelt, 2016). This oversupply of nutrients can lead to  
37    eutrophication and subsequent loss of biodiversity. With the aim of ensuring the long-term survival of  
38    Europe's most valuable and threatened species and habitats, the Natura 2000 network of protected areas  
39    (EEA, 2017) was established in Europe under the 1992 Habitats Directive (EU, 1992). While it is



40 estimated that only 7% of the total EU-28 ecosystem area and 5% of the Natura 2000 area was at risk of  
41 acidification in 2010 (EEA, 2015), it is estimated that the fraction exposed to air-pollution levels  
42 exceeding eutrophication limits is 63% and 73%, respectively, in 2010 (EEA, 2015).

43  
44 The Task Force on Hemispheric Transport of Air Pollution (HTAP) under the UNECE Convention on  
45 Long Range Transport of Air Pollution program (CLRTAP) has organized several modeling exercises to  
46 understand the role of hemispheric transport when estimating the impacts of remote sources on  
47 background concentrations and deposition in different parts of the world (Galmarini et al. 2017). A  
48 description of the HTAP program can be found at [www.htap.org](http://www.htap.org). While early exercises used global  
49 models, the most recent research activity, HTAP2, foresees a combination of global and regional models,  
50 in order to evaluate air pollution impacts at a higher spatial resolution. In this context, the project  
51 AQMEII (Air Quality Model Evaluation International Initiative, Rao et al. 2009) in its third phase activity  
52 (AQMEII 3) has brought together various air quality modelling teams from North America and Europe to  
53 conduct a set of the simulations under the HTAP framework (Solazzo et al. 2017). At the same time, the  
54 EURODELTA-Trends (EDT) project has also brought together several European modeling teams, to  
55 provide information for the Task Force on Measurements and Modelling (also under the CLRTAP),  
56 including the evaluation of models for specific campaigns (Bessagnet et al. 2016; Vivanco et al, 2016),  
57 and, more recently, for 20-year trends of air quality and deposition (Colette et al. 2017). Since both  
58 projects have a model evaluation component and there is a common simulation year (2010), it is possible  
59 to evaluate the datasets jointly, enabling the comparison of a larger number of models (eight for  
60 AQMEII3 plus seven for EDT).

61 The availability of 14-model simulations provides the possibility of obtaining a more robust ensemble  
62 model estimate of deposition than that from a single model, as well as an estimate of deposition  
63 uncertainty. This more robust estimate is particularly useful for assessing ecological impacts such as  
64 critical load exceedance. Critical loads (CL) are limits for deposition of atmospheric pollutants, set by the  
65 Working group on Effects of the CLRTAP for the protection of ecosystems (de Wit et al., 2015).  
66 Exceedances of CL have been utilized during the last decades to assess impacts of atmospheric pollution  
67 to natural and semi-natural European ecosystems. Moreover, applying empirical CL for the nutrient N is  
68 recommended to assess “whether N deposition should be listed as a threat to future prospects” in the  
69 framework of the Habitats Directive 92/43/EEC (Henry and Aherne, 2014; Whitfield et al., 2011).

70 In addition to a model evaluation, we include an estimation of the exceedances of CL for the habitats in  
71 the European Natura 2000 network most threatened by N deposition. Moreover, in addressing one of the  
72 objectives of HTAP (Galmarini et al., 2017), we estimated the changes in wet deposition in Europe due to  
73 1) a reduction of global emissions by 20% or to a regional 20% emission reduction solely in 2) North  
74 America or 3) Europe.

75 The paper is divided into four main sections. Section 2 focuses on the evaluation of model performance  
76 for wet deposition in 2010 (the base case scenario in the context of HTAP and AQMEII3). Section 3  
77 presents the intercomparison of dry deposition. Section 4 provides an overview of the exceedances of the  
78 CL for the most threatened habitats in the Natura 2000 network considering the results of an ensemble,  
79 and finally, Section 5 includes an assessment of the influence of 20% emission reductions alternatively in  
80 Europe, North America and at a global scale on deposition in Europe.



81 **2 Model evaluation and intercomparison of wet deposition estimates**

82 **2.1 Methodology**

83 This Section describes the model simulations (2.1.1), the observations used for model evaluation (2.2.2)  
84 and the procedure to evaluate model performance (2.1.3).

85 Table 1 shows the description and abbreviations of the variables used in the assessment.

86

87 **2.1.1 Model simulations**

88 The simulations for the year 2010 used in this study were carried out using 14 air quality models (Table  
89 2), seven of them as part of AQMEII3, and the other seven models participating in EDT. CHIMERE was  
90 involved in both projects, although the model version used in the EDT project is an improved (not yet  
91 official) version (Chimere2017b v1.0), and therefore a direct comparison of model results between both  
92 simulations (AQMEII3 and EDT) is not possible. More modelling teams than those in Table 2 were  
93 involved in the AQMEII3 project, but we kept only those that provided all the variables required for the  
94 model performance evaluation in terms of wet deposition, i.e. air concentrations and deposition of related  
95 chemical species (except AQ\_TR1\_MACC, which only provided deposition data). The domain and grid  
96 resolution was common for all the models in EDT (except for ED\_CMAQ, which used a different  
97 domain/projection), with a resolution of  $0.25^\circ$  (lat)  $\times$   $0.4^\circ$  (lon). AQMEII3 permitted a more flexible  
98 model setup, although outputs had to be produced for a fixed domain with a spatial resolution of  $0.25^\circ \times$   
99  $0.25^\circ$ . Meteorological inputs for the AQMEII3 models were chosen by each participant (Table 2). In  
100 EDT, meteorological inputs from the Weather Research and Forecast model (WRF 3.3.1) were provided  
101 centrally, although not all models used this common dataset (WRF-Common). In both exercises,  
102 boundary conditions were provided to the participants; in AQMEII3 they come from a global model, C-  
103 IFS(CB05) (Flemming et al., 2015) running the same scenarios. In EDT boundary conditions come  
104 primarily from observations combined with optimal interpolation and long term trends, following the  
105 procedure used in the EMEP model (Simpson et al., 2012), with slight adjustments in the context of trend  
106 modelling (Colette et al., 2017). Emissions were also fixed in both projects: In AQMEII3 two options  
107 were available, Copernicus emissions or HTAP\_v2.2 emissions (Janssens-Maenhout, 2015) which for the  
108 European region actually contain the Copernicus inventory. In EDT they are ECLIPSE\_V5 emissions  
109 estimated by the GAINS (Greenhouse gases and Air pollution INteractions and Synergies) model (Amann  
110 et al., 2011). More information on the model setups can be found in Galmarini et al. (2017) and Solazzo  
111 et al. (2017) for AQMEII3 and Colette et al. (2017) for EDT.

112 Four simulations were carried out by the AQMEII3 community: a base case (BAS) for 2010; GLO, where  
113 emissions were reduced at a global level by 20%; EUR, where emissions were reduced in Europe by 20%  
114 and NAM, where emissions were reduced in North America by 20%. Not all the models performed the  
115 simulations for all four cases.

116 **2.1.2 Observations**

117 Measurements (annual and monthly) made at 88 EMEP monitoring sites for 2010 were provided by the  
118 Norwegian Institute for Air Research (NILU), which is the Chemical Coordinating Centre of EMEP,



119 although not all variables were measured at all sites. A complete description of the monitoring network of  
120 the EMEP program, as well as the sampling methodologies used can be found in Tørseth et al (2012) and  
121 the data are openly accessible from <http://ebas.nilu.no/>. A summary of sites and variables considered is  
122 included in Table 3 and a map with their location is given in Fig. 1. Measurements for the gas phase  
123 ( $\text{HNO}_3$ ,  $\text{NH}_3$ ) are quite scarce, which makes it difficult to evaluate models performance for these species.  
124 For example, for annual values, more than two thirds of the sites had measurements for both N and S  
125 deposition and atmospheric  $\text{SO}_2$  concentrations, while only 10% had data for air concentrations of  $\text{HNO}_3$   
126 and  $\text{NH}_3$ . More sites than those for  $\text{HNO}_3$  and  $\text{NH}_3$  are measuring inorganic aerosols, through these are  
127 analyzed from of  $\text{PM}_{10}$  samples in addition to the filterpack which sample both aerosols and gases. One  
128 should be aware that the  $\text{NH}_4^+$  and  $\text{NO}_3^-$  concentrations might be underestimated due to the evaporation of  
129 ammonium nitrate. This is the case for both  $\text{PM}_{10}$  and filterpack measurements, where the separation of  
130 the nitrogen gases might be biased. The sum of  $\text{HNO}_3$  and  $\text{NO}_3^-$ , as well as the sum of  $\text{NH}_3$  and  $\text{NH}_4^+$  are  
131 however considered unbiased. The filterpack samplers usually have no size cut off, but can be considered  
132 to be around  $\text{PM}_{10}$  (EMEP, 2014).  
133 The spatial coverage of the observations used in the evaluation is quite high for most of northern, central  
134 and Western Europe, including Spain, but is quite low in the eastern and southern regions (Fig 1).

### 135 2.1.3 Evaluation

136 Model evaluation involved a joint analysis of wet deposition and air concentrations of the corresponding  
137 gas and particle species, as well as precipitation. Accumulated values were considered for precipitation  
138 and wet deposition, whereas mean values were used for air concentrations. Both annual and monthly  
139 values were evaluated. For each model simulation, the following statistics were calculated (Table 4):  
140 normalized mean squared error (NMSE), fractional bias (FB) and the fraction of model estimates within a  
141 factor of two of the observed values (FAC2). The acceptance criteria proposed by Chang and Hanna  
142 (2004; 2005) were used to assess model acceptability: that is, FAC2 higher or equal to 0.5, values of FB  
143 between -0.3 and 0.3, and NMSE values lower than or equal to 1.5. We define a model as performing  
144 acceptably for a particular variable, when two out of these three criteria are met; in recognition of the  
145 large uncertainties involved in these types of simulations. It should be noted that the acceptability criteria  
146 adopted in this study had their origin in evaluating Gaussian atmospheric dispersion models rather than  
147 photochemical Eulerian grid models. However, due to the absence of established performance criteria for  
148 evaluating modeled atmospheric deposition, these criteria were nevertheless adopted in this study while  
149 future work may be directed at developing performance goals more specifically tailored towards  
150 atmospheric deposition. To illustrate model performance for each variable, the three assessment statistics  
151 are shown on the same graph by plotting NMSE against FB and using a different symbol to indicate  
152 whether a model meets the acceptance criterion of Chang and Hanna (2004) for FAC2 ( $\text{FAC2} \geq 0.5$ ).  
153 These plots include shaded areas that correspond to areas meeting the acceptance criteria of Chang and  
154 Hanna (2004) (blue for NMSE, red for FB). In addition, the theoretical minimum NMSE for a given value  
155 of FB is also plotted (parabolic dashed lines) (Chang and Hanna, 2004). These “smile plots”, as they are  
156 called hereafter, were produced considering annual and monthly data, and also by month, in order to  
157 illustrate the seasonal behavior. All statistics were calculated in two ways: 1) independently for each



158 variable, so as to have the largest number of available sites for each variable, and 2) considering a  
159 common set of sites for wet deposition and air concentrations of the respective gas and particle species for  
160 each deposition type: oxidized nitrogen (ON), reduced nitrogen (RN) and sulfur (S).

161 Additional statistics, (mean gross error, MGE, normalized mean bias, NMB, normalized mean gross error,  
162 NMGE, root mean squared error, RMSE, correlation coefficient,  $r$ , coefficient of efficiency, COE and  
163 index of agreement, IOA), were also calculated, as defined in the Auxiliary material (AM 3.9).

164 In order to provide robust estimates of N and S deposition and their uncertainties for further applications,  
165 such as the one in Section 4, a multi-model ensemble was constructed using the mean and standard  
166 deviation of the total deposition for each grid cell calculated from the estimates of the best performing  
167 models. A given model was included if it met at least two of the three acceptability criteria for wet  
168 deposition, gas and particle concentration, considering results for all the available sites and common sites.  
169 The main problem with this approach was that gas concentrations of NH<sub>3</sub>\_N and HNO<sub>3</sub>\_N were only  
170 measured at a few measurements sites. When the criteria for these gas pollutants were the only ones  
171 failing, we retained the model (ED\_EMEP, AQ\_FI\_MACC&HTAP) if the criteria for total concentrations  
172 was met (note that TNO<sub>3</sub> and TNH<sub>4</sub> were measured at some sites where no separate measurements of gas  
173 and particle air concentrations were made and thus model performance for these variables as well as  
174 TSO<sub>4</sub> was only evaluated for all available sites).

175  
176

## 177 **2.2 Results and discussion**

178 The evaluation statistics for the selected models are provided in the tables in AM 3.6. These results are  
179 represented visually in the *smile plots* of Fig. 2 (based on annual values, considering all the available sites  
180 for each variable) and AM 3.1 (based on monthly values), which also show the degree to which the  
181 acceptability criteria were met for all models. Fig. 3 shows the *smile plots* considering only the common  
182 set of sites (sites with measurements of all the variables), to facilitate the analysis with regards to the  
183 interdependencies of model performance for different variables. Results for the ensemble, calculated as  
184 exposed in Section 2.1.3 are also included in smile plots and tables, in order to have a view of the quality  
185 of its performance. Considering the criteria in Section 2.1.3 and tables AM 3.7 (calculated for all the  
186 available sites) and 3.8 (for common sites) jointly (that is, the criteria had to be met in both tables, on an  
187 annual basis), the ensemble was composed of AQ\_DK1\_HTAP, ED\_CHIM, ED\_EMEP, ED\_LOTO,  
188 AQ\_FI1\_MACC, AQ\_FI1\_HTAP and ED\_MATCH for N deposition (considering both ON and RN at  
189 the same time; gridded information for AQ\_UK1\_MACC and AQ\_UK2\_HTAP, passing the acceptance  
190 criteria, was not available). For S deposition the models meeting the criteria for SO<sub>2</sub>\_S, PM\_SO<sub>4</sub>\_S and  
191 WSO<sub>4</sub>\_S were ED\_EMEP, ED\_LOTO, ED\_MATCH, AQ\_FI1\_HTAP, AQ\_FI1\_MACC and  
192 AQ\_UK1\_MACC (AQ\_UK1\_MACC gridded information was not available for all the variables, so it  
193 was not included in the ensemble). Figs. 4 and 6 show the deposition of N and S for the selected models  
194 and the ensemble. The ensemble was calculated to facilitate the analysis in Section 4. Maps of annual wet  
195 deposition for all the models are shown in AM 1. Other criteria to select the models in the ensemble or the  
196 way to calculate it would lead to a different ensemble.



197 Accumulated precipitation was also evaluated. In general, monthly and annual precipitation rates  
198 estimated by the models agree reasonably well with the observations. The *smile plots* for precipitation in  
199 Fig. 2 and AM 3.1 (and the tables in the AM 3.6) show that all the models meet all acceptability criteria,  
200 with the exception of AQ\_DE1\_HTAP, which narrowly misses the FB criterion for this variable.  
201 AQ\_FRES1\_HTAP had the lowest errors (NMSE) and the highest correlation with the observed  
202 precipitation values ( $r$ ).

203 In the case of WNO<sub>3</sub>\_N (abbreviations in Table 1) a large variability was found (AM 1.2), with  
204 ED\_MINNI and AQ\_DE1\_HTAP giving the lowest values and AQ\_TR1\_MACC giving the highest. The  
205 *smile plot* in Fig. 2 (also included in AM 1.2 to facilitate interpretation) and tables in AM 3.6 show that  
206 the models tended to underestimate the observed WNO<sub>3</sub>\_N, (ED\_EMEP and AQ\_DK1\_MACC very  
207 slightly underestimating), on average, with the exception of AQ\_TR1\_MACC and ED\_MATCH, that  
208 overestimated slightly. The results for ED\_MINNI are consistent with the study by Vivanco et al. (2016),  
209 who evaluated several models (EMEP, CHIMERE, LOTOS-EUROS, MINNI, CMAQ and CAMX) for  
210 four one-month campaigns during 2006, 2007, 2008 and 2009. Most of the models meet at least two of  
211 the three acceptability criteria for both monthly and annual wet deposition values, with the exceptions  
212 being ED\_MINNI and AQ\_DE1\_HTAP, which substantially underestimated deposition. As shown in  
213 AM 3.6 all the models performed acceptably for TNO<sub>3</sub>\_N, except AQ\_DE1\_HTAP for the monthly data  
214 and ED\_CMAQ for the annual data. Interestingly, all the models performed worse for atmospheric  
215 concentration of the gaseous form (HNO<sub>3</sub>\_N) than for the particulate form (PM\_NO<sub>3</sub>\_N) (also visible in  
216 Fig. 3), with no model performing acceptably for the monthly data. Boxplots in AM 4 indicate an  
217 underestimation of the HNO<sub>3</sub>:TNO<sub>3</sub> ratio in winter for most of the models. The *smile plots* in the AM 3.2  
218 also show the highest errors and underestimation of HNO<sub>3</sub>\_N during these months. In fact, no model  
219 meets two criteria in Jan, Feb, Mar, Nov and Dec for this pollutant. Most models overestimated HNO<sub>3</sub>\_N  
220 in the period May-Sep, with the exception of July for which the models tended to underestimate  
221 concentrations. This summer period was also when the models estimated the highest HNO<sub>3</sub>:TNO<sub>3</sub> ratios,  
222 many of which were higher than observed (especially for AQ\_FRES1\_HTAP, ED\_MINNI). The models  
223 performed best for the gaseous component during Jun-Aug. Most models underestimate both WNO<sub>3</sub>\_N  
224 and HNO<sub>3</sub>\_N and overestimate PM\_NO<sub>3</sub>\_N for the winter period (Oct-Mar), which could suggest a too  
225 efficient gas-to-particle conversion during these months in some cases, with maybe low deposition  
226 efficiency for the particle phase. In the case of AQ\_DE1\_HTAP the underestimation of deposition, as  
227 well as gas and particle air concentration could be related to an underestimation of NO<sub>2</sub> or HNO<sub>3</sub> (via a  
228 low NO<sub>2</sub> to HNO<sub>3</sub> conversion rate). ED\_EMEP overestimates WNO<sub>3</sub>\_N and PM\_NO<sub>3</sub>\_N, but  
229 underestimates HNO<sub>3</sub>\_N (according to annual values for common sites in AM 3.8), which could be  
230 related to a too high gas deposition.

231 For WNH<sub>4</sub>\_N there were also large differences between the models giving the lowest values  
232 (AQ\_DE1\_HTAP, AQ\_FRES1\_HTAP and ED\_MINNI), and the models giving the highest  
233 AQ\_TR1\_MACC). Most of the models meet at least two of the three acceptability criteria for this  
234 pollutant, with the exceptions being AQ\_DE1\_HTAP, AQ\_FRES1\_HTAP and ED\_MINNI. Similar to  
235 WNO<sub>3</sub>\_N, Fig. 2 (also included in AM 1.1) and tables in AM 3.6 show that the models tended to  
236 underestimate WNH<sub>4</sub>\_N, with the exception of AQ\_TR1\_MACC and ED\_MATCH. However, unlike



237 WNO<sub>3</sub>\_N, this underestimation seems to correlate with an overestimation of the gaseous form (NH<sub>3</sub>\_N)  
238 on an annual basis (except for ED\_EMEP, which has a very low bias for both pollutants and  
239 ED\_MATCH, which overestimates WNH<sub>4</sub>\_N slightly). This is likely due to an underestimation of wet  
240 removal processes for the gas phase, but it can also be related to other issues, such as a general  
241 underestimation of NH<sub>3</sub> dry deposition or an overestimation of emissions or even to measurement  
242 locations far from agricultural sources of ammonia and therefore not representative of the grid square.  
243 The overestimation of NH<sub>3</sub>\_N mainly occurs in autumn and winter (Jan, Feb, Nov, Dec), as can be  
244 inferred from the monthly *smile plots* of NH<sub>3</sub>\_N in the AM 3.3, which shows a poorer model  
245 performance for this period (no model meets all three criteria). It is interesting to see that this  
246 overestimations of NH<sub>3</sub>\_N during Nov-Jan takes place when HNO<sub>3</sub>\_N is underestimated, which could  
247 indicate an excessive conversion of HNO<sub>3</sub> to particle due to an excess of NH<sub>3</sub> (aerosol nitrate may be  
248 formed if enough ammonia is available) and favored with low temperatures. Ammonium is quite well  
249 reproduced, with all the models meeting the acceptance criteria both on an annual basis and a monthly  
250 basis. All in all, tables in AM 3.6 indicate a general underestimation of wet deposition for reduced  
251 nitrogen, with a tendency to overestimate TNH<sub>4</sub>. There is more variability between the model estimates  
252 of the NH<sub>3</sub>:TNH<sub>4</sub> ratios for the winter months (AM 4) with the EDT models estimating lower ratios. It  
253 should be noted that some models do not distinguish between precipitation types and use the same  
254 scavenging rates for snow and rain, which could lead to substantial differences between model results.  
255 Substantial differences were also found for WSO<sub>4</sub>, from the lowest values for ED\_CHIM up to the  
256 highest for AQ\_TR1\_MACC and ED\_MATCH. Most of the models meet at least two of the three  
257 acceptability criteria for WSO<sub>4</sub>, apart from AQ\_DK1\_HTAP, AQ\_FRES1\_HTAP, ED\_CHIM and  
258 ED\_MINNI. Similar to the N deposition, the models tended to underestimate the observed values (Fig. 2),  
259 with the exception of AQ\_TR1\_MACC, AQ\_UK2\_HTAP, ED\_EMEP and ED\_MATCH. The tendency  
260 to underestimate WSO<sub>4</sub>\_S by most models, and similarly to the reduced nitrogen, is overall occurring  
261 simultaneously with an overestimation of the gaseous pollutant (SO<sub>2</sub>\_S) on an annual and monthly basis.  
262 As shown in the monthly *smile plots* in the AM 3.4, the models generally underestimate WSO<sub>4</sub>\_S for all  
263 months although the bias tends to be smaller (and even positive for some models) during the winter  
264 period (Nov-Feb). The bias for SO<sub>2</sub>\_S does not have a seasonal cycle and the largest errors occur in Mar,  
265 Jun and Nov. Model performance is generally better for the particulate concentrations (PM\_SO<sub>4</sub>\_S)  
266 although some large errors occur in the winter (Nov-Jan). All models tended to overestimate TSO<sub>4</sub>, with  
267 the exception of ED\_CHIM, ED\_EMEP and ED\_LOTO, and most models also tended to overestimate the  
268 SO<sub>2</sub>:TSO<sub>4</sub> ratios.

269 In summary, and considering the whole picture, wet deposition fluxes are generally underestimated for  
270 WSO<sub>4</sub>\_S and WNH<sub>4</sub>\_N, and in winter in the case of WNO<sub>3</sub>\_N. There are indications that the aqueous  
271 and heterogeneous chemistry (e.g. those involving conversion of NO<sub>x</sub> to HNO<sub>3</sub>) could be too slow or  
272 under-represented in the models, especially in winter, evidenced by an overestimation of primary gaseous  
273 pollutants, especially NH<sub>3</sub> and SO<sub>2</sub> for this period and an underestimation of the secondary pollutant  
274 HNO<sub>3</sub> (also formed via heterogeneous chemistry). However, this behavior (simultaneous overestimation  
275 of NH<sub>3</sub>\_N and underestimation of HNO<sub>3</sub>\_N in winter) could also be due to an excessive formation of  
276 nitrates (favored by low temperatures) due to a potential excess of NH<sub>3</sub> (aerosol nitrate may be formed





277 only if enough ammonia is available). This excess NH<sub>3</sub> could be due to an overestimate of NH<sub>3</sub>  
278 emissions during these months. The fact that sulphate concentration is also low for several models in Jan  
279 and Feb and SO<sub>2</sub> somewhat high could be due to an underestimate of the conversion to aerosol (sulphate)  
280 via aqueous chemistry, which could be another cause of the excess NH<sub>3</sub>.

### 281 **3 Model intercomparison of dry deposition**

282 Figures in AM 2 show maps of dry deposition for oxidized nitrogen (OND) (AM 2.2), reduced nitrogen  
283 (RND) (AM 2.1), total N (ND) (AM 2.4) and S (AM 2.5). Unfortunately, not all the models participating  
284 in AQMEI3 provided the complete set of outputs, and therefore it was not possible to study the estimated  
285 dry deposition for all of them. Maps of dry deposition of total N (ND) for all the models show the highest  
286 values over France, Germany and other areas in the center of the domain. Differences between models  
287 can be seen in both high and low emission areas. Models have different deposition algorithms and, even  
288 when similar, they can have different input, such as land use or the leaf index area. It would be interesting  
289 in future studies to analyse how much different these parameters in the models are, due to their relevant  
290 importance in dry deposition estimates. The highest values of dry deposition for total N (AM 2.4) are  
291 found for ED\_CMAQ, with values higher than 1900 mg N m<sup>-2</sup> (annual accumulated value) over large  
292 areas in the central and western parts of the domain and mainly due to the contribution of the oxidized  
293 species. AQ\_FRES1\_HTAP estimated the lowest values whereas the rest of model estimates have more  
294 similar spatial patterns. Significant differences can be found when looking at the gas and particle  
295 deposition for the AQMEI3 participants. Two gases, NO<sub>2</sub> and HNO<sub>3</sub> can contribute to OND. As can be  
296 inferred from AM 2.3, AQ\_DK1\_HTAP estimate the main contribution from the gas phase, whereas in  
297 the case of AQ\_TR1\_MACC, highest contributions to OND come from the particle phase. This highlights  
298 the importance of making measurements that can shed more light on these processes, providing modelers  
299 with data that can be used to parameterize and evaluate the different processes. For RN only  
300 AQ\_FRES1\_HTAP, AQ\_UK2\_HTAP and AQ\_FI1\* in AQMEI3 provided the information required to  
301 calculate RND. The models estimate similar spatial distributions of RND, with the highest values in the  
302 Netherlands, the western part of France, Denmark and Belgium, as well as some high values in the area of  
303 the Alps. Spatial distributions are also similar for dry deposition of S (AM 2.5; higher values mainly over  
304 Poland, The Netherlands, United Kingdom, Germany and Southeastern Europe), although in this case  
305 with higher differences in values, as it can be inferred from maps in AM 2.5. ED\_CMAQ presents a  
306 different spatial pattern, with high values also over sea, due to the consideration of sulfates coming from  
307 sea salt in this model application.

308

### 309 **4 Deposition of N over areas in Nature 2000 network**

310 In this section, we first analyze the representativeness of the monitoring sites used in the evaluation of  
311 model deposition with a focus on habitat conservation. Secondly, the estimated deposition by the multi-  
312 model ensemble is used to evaluate the total N deposition (dry + wet) to the protected habitats. Finally, a  
313 simple evaluation (where possible) of the CL exceedances is presented. Together with S deposition, N  
314 deposition also contributes to acid deposition. However, as mentioned in the introduction, only 5% of the



315 Natura 2000 area was at risk of acidification in 2010 and so the focus of this part of the study is on the  
316 exceedances of CLs for the nutrient N.

317

#### 318 **4.1. Representativeness of monitoring sites for conservation purposes**

319 The EMEP measurements are regional representative (Tørseth et al 2012 , EMEP, 2014) and have  
320 historically been considered to represent an area larger than the size resolution of the EMEP atmospheric  
321 dispersion model (for the grid with 50x50km<sup>2</sup> of horizontal resolution). This resolution was taken as a  
322 reference for establishing a buffer zone of 2500 km<sup>2</sup> around the receptors. The protected habitats inside  
323 the buffer zone were determined by intersecting the surface area of the Natura 2000 network (EEA,  
324 2017), with the cover of the most-likely habitats in Europe using EUNIS level-1 classification (EEA,  
325 2015). Previously to this, aquatic, aquatic-related and anthropic habitats (such as gardens or arable lands)  
326 were excluded, in order to study only natural and semi-natural terrestrial ecosystems. The surface area  
327 covered by each habitat class included in the Natura 2000 network was plotted against the surface area of  
328 the same protected habitat classes within the above-mentioned buffer zones, in relative values with  
329 respect to their respective totals (Table 5, Fig. 8). The most represented terrestrial habitats in the entire  
330 network are broadleaved deciduous woodland, coniferous woodland, mesic grasslands and mixed  
331 deciduous and coniferous woodland (EUNIS classifications G1, G3, E2 and G4, respectively). The results  
332 indicate that the selected monitoring sites represent the main classes of terrestrial habitats fairly well, with  
333 G4 deviating most, with an overrepresentation of 51% within the protected buffered area with respect to  
334 the entire Natura 2000 network.

335 The same exercise was performed using only monitoring sites measuring all N species (including in  
336 precipitation, gaseous and particulate N). Only 8 monitoring sites, distributed between the United  
337 Kingdom, Switzerland and Eastern Europe, have the complete set of N pollutant measurements. Since the  
338 Natura 2000 network has no presence in Switzerland, only 6 sites could be evaluated for  
339 representativeness. Among the most represented habitats, G1 and G3 deviated the most in their  
340 representation. In any case, this subset can be considered small and poorly distributed across Europe.  
341 Therefore, the evaluation of model results for total concentration and deposition of N pollutants in Europe  
342 is still far from being representative in terms of conservational purposes.

#### 343 **4.2. Risk assessment of atmospheric N deposition in the Natura 2000 network**

344 The mean and standard deviation (SD) for total deposition of N obtained from the ensemble model were  
345 combined with revised empirical CL (Bobbink and Hetteling, 2011) to provide a risk assessment of N  
346 deposition effects on vegetation in the Natura 2000 network. This evaluation constitutes a first approach,  
347 which helps to locate the most-likely areas and major terrestrial habitat classes at risk of eutrophication as  
348 a result of atmospheric N deposition. Further research (particularly on habitat specific CL) and a wider  
349 monitoring network (particularly to evaluate models' performance for dry deposition) are needed to carry  
350 out a more accurate risk assessment. It is also interesting to bear in mind that even though recent studies  
351 (e.g. Cape et al., 2012; Izquieta-Rojano, 2016; Matsumoto et al., 2014) have highlighted the important  
352 contribution of the organic form to total N deposition (from 10 to more than 50%), there are still  
353 important gaps in our knowledge of the role of organic fraction in the N cycle and scarce attempts to



354 include it in the measurement networks (e.g. Walker et al., 2012). Deposition of dissolved organic N  
355 constitutes another variable involving uncertainty in the actual understanding of the N cycle (Izquieta-  
356 Rojano et al., 2016) and, consequently, in the risk assessment of N deposition. Further research is  
357 therefore needed to understand the role that organic N plays in ecosystem functioning, biogeochemical  
358 cycles and even human health.

359

360 Ensemble deposition maps were projected and resampled to coincide with the EUNIS habitat grid (level 1  
361 classification; ETRS89 LAEA projection; 100 m × 100 m cell size). The mean±SD values were used as  
362 estimates of lower and upper uncertainty limits for the deposition, which were then compared to the mean  
363 CL attributed to each habitat class (Table 5; based on those from Bobbink and Hetteling, 2011). Those  
364 areas in which the class-attributed CL was exceeded by any of the values (mean-SD; mean; mean+SD)  
365 were identified. The area presenting exceedances of empirical CL ( $CL_{exc}$ ) was summed for each EUNIS  
366 level-1 habitat class (Table 5). The areas showing  $CL_{exc}$  were mapped for the most threatened habitat  
367 classes (Fig. 9). In the case of similar habitats with similar distributions, a joint map is shown (D1 and  
368 D2; G3 and G4). Values of  $CL_{ex}$  in Fig. 10 indicate the area exposed to an exceedance of the CL  
369 expressed as percentage of the total area evaluated for each particular habitat class. These values were  
370 also calculated considering the total deposition of N from AQ\_FI\_MACC, as this model was used to  
371 estimate the variation in deposition due to changes in emissions, as it will be later explained. All these  
372 operations were performed using ArcGIS 10.2 (ESRI, Redlands CA, USA).

373 The six habitats with the largest surface area with a mean ensemble deposition above their respective CL  
374 were “alpine and subalpine grasslands” (E4), “coniferous woodlands” (G3), “mixed deciduous and  
375 coniferous woodlands” (G4), “raised and blanket bogs” (D1), “artic, alpine and subalpine scrub” (F2) and  
376 “valley mires, poor fens and transition mires” (D2), with critical load exceedances covering 65%, 34%,  
377 32%, 24%, 16% and 11% of their respective areas (Table 5). Alpine and subalpine grasslands were also  
378 detected as the types most jeopardized by N deposition, in a similar study for Spanish protected areas  
379 using 2008 simulations from EMEP and CHIMERE models (García-Gómez et al., 2014). These habitats  
380 are usually located in areas with complex topography, where model estimates of atmospheric deposition  
381 can be more spatially inaccurate, as suggested in previous studies (e.g. García-Gómez et al., 2014;  
382 Simpson et al., 2006). The scarcity of monitoring sites at high altitude to evaluate model simulations can  
383 be considered as a major uncertainty in the risk assessment for N deposition.

384 The variation among the models included in the ensemble, represented here by the standard deviation  
385 (SD) of the ensemble, mostly affected E4 (Table 5). The reduction of the area at risk of this habitat class  
386 is remarkable high (-50%), when the lower limit of the deposition is used (mean-SD; Table 5). This might  
387 indicate that the CL is exceeded in most areas by a narrow margin. Within the other five habitat classes  
388 with the highest  $CL_{exc}$  area, the area at risk decreased by 13% and increased by 16% on average, when the  
389 lower and upper limits of deposition are used. These same six habitats were again found to present the  
390 largest areas showing  $CL_{exc}$ , when using AQ\_FI1\_MACC estimates, although some differences were  
391 found (seen Figure 10).

392 Apart from the uncertainty in modelled deposition, the uncertainty in the CL attributed to the habitat  
393 classes should also be considered. On the one hand, some CL proposed in the CLRTAP revision are based



394 on expert judgment (e.g. those for E2, F5 or G4) and some were averaged from those proposed for several  
395 subclasses (e.g. for E1 and F4). On the other hand, even when the proposed CL are reliable and match  
396 perfectly with the habitat classes evaluated in this study, an adjustment linked to more local conditions is  
397 recommended (e.g. for D1 it is recommended to vary the applied CL as a function of the precipitation  
398 range or the water table level). However, since a CL averaged from the proposed range was used for each  
399 habitat class and the evaluation was performed on a broad scale, we consider that the results are suitable  
400 for the purpose of this work, which is highlighting the protected areas and terrestrial habitats with the  
401 highest probability of suffering eutrophication. Finally, the use in this approach of a modelled dry  
402 deposition that is in fact weighted for the different land use inside each grid cell might lead to an  
403 underestimation of, for instance, forests risks, as the dry deposition for plant surfaces is higher than for  
404 other land uses, and it is currently smoothed during the weighting process. To perform a more accurate  
405 assessment, habitat-type-specific values for dry deposition of N are necessary. It is, therefore,  
406 recommended that chemical transport models provide dry deposition data as a function of leaf area index  
407 (LAI) or habitat type in order to be more suitable for risk assessment studies.

408

## 409 **5 Contribution to N and S deposition in Europe of different regions (NA, EU, GLO)**

### 410 **5.1 Methodology**

411 As we have previously described in the framework of AQMEII3 activities, and to give scientific support  
412 to the HTAP task force, research activities have included an evaluation of the influence of a reduction of  
413 emissions in some parts of the Northern Hemisphere on the air quality other regions. Along these lines,  
414 some models ran simulations with 1) a 20% reduction of global emissions (GLO), 2) a 20% reduction of  
415 emissions in Europe (EUR) and 3) a 20% reduction of emissions in North America (NAM). According to  
416 the acceptance criteria described in Section 2, and the availability of models running the different  
417 emission scenarios, we chose AQ\_FI1\_MACC as a representative model to demonstrate the effects of the  
418 different emission reduction scenarios. For WNO<sub>3</sub> the results from the AQ\_FRES1\_HTAP model were  
419 included as well, as this model performed acceptably for this pollutant and simulated the three  
420 perturbation scenarios.

421 The effect of each scenario was calculated in terms of deposition (mgN/m<sup>2</sup>) and percentage changes with  
422 respect to the base case (%). Differences between the base case simulation (no emission reduction) and  
423 the different scenarios were calculated for wet and dry deposition of ON, RN and S, as well as for total  
424 deposition of N and S.

425

### 426 **5.2 Results**

427 Maps reflecting the effect of the reduction of 20% of emissions in the different scenarios are included in  
428 figures 11 and 12, for total N and S (including both oxidized and reduced N, as well as wet and dry  
429 deposition), in absolute and relative terms. In general, a 20% reduction of total N and S deposition is  
430 found when global emissions are reduced by 20% (although somewhat lower for N in the United  
431 Kingdom, the Netherlands and in Belgium). When a 20% emission reduction is only applied in Europe,



432 the deposition of N and S is decreased by 10-20%. When emissions are reduced in North America only,  
433 deposition at the eastern areas of the domain is reduced by about 2%, (Fig. 9). Im et al. (2017) found also  
434 an almost linear response to the change in emissions for NO<sub>2</sub> and SO<sub>2</sub> air concentration, for the global  
435 perturbation scenario, with slighter smaller responses for the European perturbation scenario and very  
436 small influence of the long-range transport, noticeable close to the boundaries.

437 Similar maps for wet and dry deposition are presented in AM 5 and AM 6, for wet and dry deposition.  
438 For WNO<sub>3</sub>\_N the global emission reductions have the largest effect on European deposition, with the  
439 largest changes in wet deposition in the Alpine area (North Italy, Southern Germany). These areas are  
440 also affected in terms of WNH<sub>4</sub>\_N, although in this case the emission reduction affects larger areas in  
441 Germany and The Netherlands. For WSO<sub>4</sub>\_S (AM) the highest impacts are found on the Balkan  
442 Peninsula, especially the south of Bulgaria, Rumania and Serbia. These quantities represent a reduction of  
443 about 20% of the base case deposition in most parts of Europe, even a bit higher for WNO<sub>3</sub>\_N in the  
444 Alpine area according to AQ\_FI1\_MACC. For AQ\_FRES1\_HTAP the reduction for WNO<sub>3</sub>\_N is lower,  
445 in the range 14-20% for the whole domain.

446 When emission reductions only occur in Europe, the changes in wet deposition are somewhat lower than  
447 for a global reduction according to AQ\_FI1\_MACC, (AM 5.1, AM 5.2). Reductions in WNH<sub>4</sub>\_N are  
448 similar to those of the global emission reduction scenario in western and central Europe, but substantially  
449 smaller in the eastern and northern parts of the domain, which are influenced more strongly by non-  
450 European emissions to the east. Larger differences are found between the global and European emission  
451 reduction scenarios for WNO<sub>3</sub>\_N, with an influence of non-European emissions that extends throughout  
452 the domain. In many countries wet deposition decreases by about 10% for the European emission  
453 reduction scenario, and a 20% reduction is only found over some central areas. The situation is similar  
454 for WSO<sub>4</sub>\_S, albeit with even larger contributions from non-European emissions. For  
455 AQ\_FRES1\_HTAP, the reduction of WNO<sub>3</sub>\_N is similar to that estimated by AQ\_FI1\_MACC, although  
456 the range of reduction is smaller. Emission reductions in NA have a very small effect on European wet  
457 deposition (around a 1-2%), with reductions mostly concentrated in the western part of the domain  
458 (Iceland, Ireland, United Kingdom, Portugal, France, Spain, Norway. This pattern is also reproduced by  
459 AQ\_FRES1\_HTAP, although the absolute changes for AQ\_FI1\_MACC are larger in the central area and  
460 smaller on the Iberian Peninsula. The effect of global emission reductions on dry deposition is similar to  
461 that for wet deposition, although the relative reductions are slightly smaller for DNO<sub>3</sub>\_N (except in the  
462 east and south of the domain) and slightly larger for DNH<sub>4</sub>\_N and DSO<sub>4</sub>\_S than for WNO<sub>3</sub>\_N,  
463 WNH<sub>4</sub>\_N and WSO<sub>4</sub>\_N, respectively (AM 5, AM 6). The differences between the relative changes in  
464 wet and dry deposition are similar for the European emission reduction scenario, although the relative  
465 change is larger for the dry deposition in the east of the domain. The influence of emission reductions in  
466 NA on the wet deposition is generally larger than that on the dry deposition.

467 Differences between the global emissions reduction scenario and the European emission reduction  
468 scenario, discounting the effect of NAM, indicate that there is an influence of emissions from other  
469 regions, especially to the east of the domain that could produce a 10% reduction in deposition over certain  
470 areas. This is in agreement with results from studies carried out within the framework of the HTAP task



471 force using global models, which estimate that 5-10% of European N deposition is the result of non-  
472 European emissions (Dentener et al., 2011; Sanderson, 2008).  
473 We also estimated how much these reductions in emissions affected the risks of N impacts in the Natura  
474 2000 areas. As can be inferred from Figure 10, there is a significant reduction in the habitat area  
475 withstanding CLexc for the scenarios GLO and EUR, compared with the base case (AQ\_FI1\_MACC).  
476 Particularly, the most jeopardized habitat types showed a reduction of more than a third in their overall  
477 threatened area. Both reduction scenarios showed almost similar values of CLexc, with only slight  
478 differences in E4 (where GLO reduction produces a slightly larger decrease in CLexc). G3 and G4  
479 habitats are the most affected, for which the exceeded area was approximately halved as a result of the  
480 emission reduction. In the case of NAM, no decrease is observed, indicating the low impact of  
481 hemispheric transport from North America to Europe, at least in terms of N deposition in 2010.6

## 482 6 Conclusions

483 A comparison of the wet and dry deposition of N and S estimated by 14 air quality models participating in  
484 the projects AQMEI3 and EURODELTAIII revealed considerable differences between the models. An  
485 evaluation of model performance was carried out, jointly considering air concentrations and wet  
486 deposition of the relevant compounds. Very few measurements of gaseous species (HNO<sub>3</sub> or NH<sub>3</sub>) were  
487 available, making it difficult to do a fair and complete evaluation. In general, most of the models meet at  
488 least two of the three acceptability criteria (NMSE < 1.5, |FB| < 0.3, FAC2 > 0.5) for both monthly and  
489 annual wet deposition values, with the exceptions of ED\_MINNI and AQ\_DE1\_HTAP, which  
490 substantially underestimated deposition. All the models performed acceptably for TNO<sub>3</sub>\_N, except for  
491 AQ\_DE1\_HTAP for the monthly data and ED\_CMAQ for the annual data. All the models performed  
492 worse for atmospheric concentrations of the gaseous form (HNO<sub>3</sub>\_N) than for the particulate form  
493 (PM\_NO<sub>3</sub>\_N), with no model performing acceptably for the monthly data, and most models  
494 underestimating the HNO<sub>3</sub>:TNO<sub>3</sub> ratio during the winter months. It is however important to note that the  
495 observations of independent NO<sub>3</sub><sup>-</sup> and HNO<sub>3</sub> are not measured with an unbiased method (same as NH<sub>3</sub>  
496 and NH<sub>4</sub><sup>+</sup>), so it is difficult to draw strong conclusions of the model performance for these compounds.  
497 For WNH<sub>4</sub>\_N, there was a general underestimation, that seems to correlate with an overestimation of the  
498 gaseous form (NH<sub>3</sub>\_N) on an annual basis (except for ED\_EMEP, which has a very low bias for both  
499 pollutants, and ED\_MATCH, which overestimates WNH<sub>4</sub>\_N slightly) mainly as a result of model  
500 estimates for autumn and winter (Jan, Feb, Nov, Dec). Similarly, to the reduced nitrogen, most models  
501 tend to underestimate wet deposition of sulfur (WSO<sub>4</sub>\_S) and overestimate the gaseous pollutant  
502 (SO<sub>2</sub>\_S) on an annual and monthly basis.  
503 Large differences were found between the dry deposition estimates of the models, highlighting the  
504 importance of obtaining measurement data to evaluate model performance. This point is important,  
505 considering the significant contribution of dry deposition to total deposition.  
506 A multi-model ensemble was constructed using the better-performing models for wet deposition (N and  
507 S) and having also estimated dry deposition. For N, the ensemble was produced as the mean of  
508 AQ\_FI1\_MACC, AQ\_FI1\_HTAP, AQ\_DK1\_MACC, ED\_EMEP and ED\_MATCH models, and was  
509 used to calculate exceedances of empirical critical loads for nitrogen for habitats in the European Natura



510 2000 network. Six habitats were identified as having critical load exceedances covering more than 10% of  
511 their total area: “alpine and subalpine grasslands” (E4), “coniferous woodlands” (G3), “mixed deciduous  
512 and coniferous woodlands” (G4), “raised and blanket bogs” (D1), “artic, alpine and subalpine scrub” (F2)  
513 and “valley mires, poor fens and transition mires” (D2), with critical load exceedances covering 60%,  
514 30%, 29%, 22%, 13% and 10% of their respective areas. The variation among the ensemble models, in  
515 terms of the standard deviation of the ensemble, mostly affected E4, with 85% of the habitat area  
516 exceeded for the upper deposition estimate. It’s important to point out that in addition to the uncertainty  
517 in modelled deposition, the CL attributed to a given habitat is also uncertain. Extending the deposition  
518 monitoring networks in European mountains would be not only beneficial for the study of atmospheric  
519 deposition, but also for model evaluation and risk assessment for these particularly threatened areas.

520

521 The reduction of 20% of emissions at global scale produces a 20% of reduction in total deposition of N  
522 and S, with the main contributor being Europe, according to the estimates of A\_FI1\_MACC model. This  
523 reduction of total deposition is directly related to a decrease of the CL<sub>exc</sub> found for the different habitats  
524 in Natura 2000 network, especially for G3 and G4, for which the exceeded area was approximately  
525 halved as a result of the emission reduction. Hemispheric transport of air pollutants from NAM has a low  
526 impact on wet deposition, mostly concentrated over the Atlantic area.

#### 527 **4 Acknowledgements**

528 CIEMAT work has been financed by the Spanish Ministry of Agriculture and Fishing, Food and  
529 Environment. The MATCH participation was partly funded by the Swedish Environmental Protection  
530 Agency through the research program Swedish Clean Air and Climate (SCAC) and NordForsk through  
531 the research programme Nordic WelfAir (grant no. 75007). The views expressed in this article are those  
532 of the authors and do not necessarily represent the views or policies of the U.S. Environmental Protection  
533 Agency

#### 534 **References**

535 Amann, M., Bertok, I., Borken-Kleefeld, J., Cofala, J., Heyes, C., Höglund-Isaksson, L., Klimont, Z.,  
536 Nguyen, B., Posch, M., Rafaj, P., Sandler, R., Schöpp, W., Wagner, F., and Winiwarter, W. (2011).:  
537 Cost-effective control of air quality and greenhouse gases in Europe: Modeling and policy applications,  
538 Environmental Modelling and Software, 26, 1489-1501, 2011.

539

540 Bessagnet, B., G. Pirovano, M. Mircea, C. Cuvelier, A. Aulinger, G. Calori, G. Ciarelli, A. Manders, R.  
541 Stern, S. Tsyro, M. Garcia Vivanco, P. Thunis, M.-T. Pay, A. Colette, F. Couvidat, F. Meleux, L. Rouil,  
542 A. Ung, S. Aksoyoglu, J.-M. Baldasano, J. Bieser, G. Briganti, A. Cappelletti, M. D’Isodoro, S. Finardi,  
543 R. Kranenburg, C. Silibello, C. Carnevale, W. Aas, J.-C. Dupont, H. Fagerli, L. Gonzalez, L. Menut, A.  
544 S. H. Prévôt, P. Roberts, and L. White (2016). Presentation of the EURODELTA III inter-comparison  
545 exercise - Evaluation of the chemistry transport models performance on criteria pollutants and joint



- 546 analysis with meteorology. Atmos. Chem. Phys., 16, 12667-12701, 2016 [http://www.atmos-chem-](http://www.atmos-chem-phys.net/16/12667/2016/)  
547 [phys.net/16/12667/2016/](http://www.atmos-chem-phys.net/16/12667/2016/) doi:10.5194/acp-16-12667-2016  
548
- 549 Bobbink R, Hettelingh JP (eds.) (2011). Review and revision of empirical critical loads and dose-  
550 response relationships. Coordination centre for effects, National Institute for Public Health and the  
551 Environment (RIVM). 244 pp. [www.rivm.nl/cce](http://www.rivm.nl/cce).
- 552
- 553 Cape, J.N., Tang, Y.S., Gonzalez-Benitez, J.M., Mitosinkova, M., Makkonen, U., Jocher, M., Stolk, A.  
554 (2012). Organic nitrogen in precipitation across europe. Biogeosciences 9, 4401-4409, doi: 10.5194/bg-9-  
555 4401-2012  
556
- 557 Chang, J.C., Hanna, S.R. (2004). Air quality model performance evaluation. Meteorol. Atmos. Phys. 87  
558 (1), 167-196.  
559
- 560 Chang, J. C., & Hanna, S. R. (2005). Technical descriptions and user's guide for the BOOT statistical  
561 model evaluation software package, version 2.0. Harmonisation within atmospheric dispersion modelling  
562 for regulatory purposes.  
563
- 564 Colette, A., Andersson, C., Manders, A., Mar, K., Mircea, M., Pay, M.-T., Raffort, V., Tsyro, S.,  
565 Couvélér, C., Adani, M., Bessagnet, B., Bergstrom, R., Briganti, G., Butler, T., Cappelletti, A., Couvidat,  
566 F., D'Isidoro, M., Doumbia, T., Fagerli, H., Granier, C., Heyes, C., Klimont, Z., Ojha, N., Otero, N.,  
567 Schaap, M., Sindelarova, K., Stegehuis, A. I., Roustan, Y., Vautard, R., van Meijgaard, E., Vivanco, M.  
568 G., and Wind, P.: EURODELTA-Trends, a multi-model experiment of air quality hindcast in Europe over  
569 1990-2010, Geosci. Model Dev., 10, 3255-3276, <https://doi.org/10.5194/gmd-10-3255-2017>, 2017.
- 570 De Wit Heleen A., Jean-Paul Hettelingh, Harry Harmens (editors) (2015) Trends in ecosystem and health  
571 responses to long-range transported atmospheric pollutants. ICP Waters report 125/2015  
572 [http://www.unece.org/fileadmin/DAM/env/documents/2016/AIR/Publications/Trends\\_in\\_ecosystem\\_and](http://www.unece.org/fileadmin/DAM/env/documents/2016/AIR/Publications/Trends_in_ecosystem_and_health_responses_to_long-range_transported_atmospheric_pollutants.pdf)  
573 [health\\_responses\\_to\\_long-range\\_transported\\_atmospheric\\_pollutants.pdf](http://www.unece.org/fileadmin/DAM/env/documents/2016/AIR/Publications/Trends_in_ecosystem_and_health_responses_to_long-range_transported_atmospheric_pollutants.pdf)  
574  
575
- 576 Couvidat, F., Bessagnet, B., Garcia-Vivanco, M., Real, E., Menut, L., and Colette, A., (2018),  
577 Development of an inorganic and organic aerosol model (Chimere2017b v1.0): seasonal and spatial  
578 evaluation over Europe, Geosci. Model Dev., 11, 165-194, <https://doi.org/10.5194/gmd-11-165-2018>  
579 <https://www.geosci-model-dev.net/11/165/2018/>  
580
- 581 Dentener, F., Keating, T. and Akimoto, H. (eds.) (2011). Hemispheric Transport of Air Pollution 2010,  
582 Part A: Ozone and Particulate Matter, Air Pollution Studies No. 17. United Nations, New York.
- 583 EEA, 2014, Effects of air pollution on European ecosystems, Past and future exposure of European  
584 freshwater and terrestrial habitats to acidifying and eutrophying air pollutants, EEA Technical report No  
585 11/2014, European Environment Agency.





586

587 EEA, 2015. Ecosystem types of Europe. 1:100000. Copenhagen: European Environment Agency (EEA).

588 Available at: <https://www.eea.europa.eu/data-and-maps/data/ecosystem-types-of-europe#tab-gis-data>.

589

590 EEA, 2017. Natura 2000 data - the European network of protected sites. 1:100000. Available at:

591 <https://www.eea.europa.eu/data-and-maps/data/natura-8#tab-gis-data>

592

593 EMEP, 2014. Manual for sampling and chemical analysis. Norwegian Institute for Air Research (NILU),

594 Kjeller, Norway. (EMEP/CCC-Report 1/2014). URL: <http://www.nilu.no/projects/ccc/manual/index.html>

595 Flemming, J., Huijnen, V., Arteta, J., Bechtold, P., Beljaars, A., Blechschmidt, A.-M., Diamantakis, M.,

596 Engelen, R. J., Gaudel, A., Inness, A., Jones, L., Josse, B., Katragkou, E., Marecal, V., Peuch, V.-H.,

597 Richter, A., Schultz, M. G., Stein, O., and Tsikerdekis, A. (2015): Tropospheric chemistry in the

598 Integrated Forecasting System of ECMWF, Geosci. Model Dev., 8, 975-1003,

599 <https://doi.org/10.5194/gmd-8-975-2015>, 2015

600

601 Galmarini, S., B. Koffi, E. Solazzo, T. Keating, C. Hogrefe, M. Schulz, Anna Benedictow, J.J.

602 Griesfeller, G. Janssens-Maenhout, G. Carmichael, J. Fu, and F. Dentener, 2017.. Technical note:

603 Coordination and harmonization of the multi-scale, multi-model activities HTAP2, AQMEII3, and

604 MICS-Asia3:simulations, emission inventories, boundary conditions, and model output formatsAtmos.

605 Chem. Phys., 17, 1543–1555, 2017

606

607 Henry J, Aherne J., (2014). Nitrogen deposition and exceedance of critical loads for nutrient nitrogen in

608 Irish grasslands. Science of the Total Environment 2014; 470–471:216–23.

609

610 Hanna, S.R., Chang, J., (2010). Setting Acceptance Criteria for Air Quality Models. Proceedings of the

611 International Technical Meeting on Air Pollution Modelling and its Application. Turin, Italy. 2010.

612

613 Im et al. Submitted to ACP

614

615 Izquieta-Rojano, S., García-Gomez, H., Aguilhaume, L., Santamaría, J.M., Tang, Y.S., Santamaría, C.,

616 Valiño, F., Lasheras, E., Alonso, R., Àvila, A., Cape, J.N., Elustondo, D. (2016). Throughfall and bulk

617 deposition of dissolved organic nitrogen to holm oak forests in the Iberian Peninsula: Flux estimation and

618 identification of potential sources. Environmental Pollution 210, 104–112, doi:

619 10.1016/j.envpol.2015.12.002

620

621 Janssens-Maenhout, G., M. Crippa, D. Guizzardi, F. Dentener, M. Muntean, G. Pouliot, T. Keating, Q.

622 Zhang, J. Kurokawa, R. Wankmüller, H. Denier van der Gon, J. J. P. Kuenen, Z. Klimont, G. Frost, S.

623 Darras, B. Koffi, and M. Li (2015): HTAP\_v2.2: a mosaic of regional and global emission grid maps for



- 624 2008 and 2010 to study hemispheric transport of air pollution. [www.atmos-chem-](http://www.atmos-chem-phys.net/15/11411/2015/doi:10.5194/acp-15-11411-2015)  
625 [phys.net/15/11411/2015/doi:10.5194/acp-15-11411-2015](http://www.atmos-chem-phys.net/15/11411/2015/doi:10.5194/acp-15-11411-2015)  
626
- 627 Maas, R., P. Grennfelt (eds), (2016). Towards Cleaner Air. Scientific Assessment Report 2016. EMEP  
628 Steering Body and Working Group on Effects of the Convention on Long-Range Transboundary Air  
629 Pollution, Oslo.  
630 [http://www.unece.org/fileadmin/DAM/env/lrtap/ExecutiveBody/35th\\_session/CLRTAP\\_Scientific Asses-](http://www.unece.org/fileadmin/DAM/env/lrtap/ExecutiveBody/35th_session/CLRTAP_Scientific_Assessment_Report_-_Final_20-5-2016.pdf)  
631 [sment Report - Final 20-5-2016.pdf](http://www.unece.org/fileadmin/DAM/env/lrtap/ExecutiveBody/35th_session/CLRTAP_Scientific Asses-)  
632
- 633 Matsumoto, K., Yamamoto, Y., Kobayashi, H., Kaneyasu, N., Nakano, T. (2014). Water-soluble organic  
634 nitrogen in the ambient aerosols and its contribution to the dry deposition of fixed nitrogen species in  
635 Japan. *Atmos. Environ.* 95, 334-343, doi: 10.1016/j.atmosenv.2014.06.037
- 636 Sanderson, M. G., Dentener, F. J., Fiore, A. M., Cuvelier, C., Keating, T. J., Zuber, A., Atherton, C. S.,  
637 Bergmann, D. J., Diehl, T., Doherty, R. M., Duncan, B. N., Hess, P., Horowitz, L. W., Jacob, D. J.,  
638 Jonson, J.-E., Kaminski, J. W., Lupu, A., MacKenzie, I. A., Mancini, E., Marmer, E., Park, R., Pitari, G.,  
639 Prather, M. J., Pringle, K. J., Schroeder, S., Schultz, M. G., Shindell, D. T., Szopa, S., Wild, O., and  
640 Wind, P. (2008): A multi-model study of the hemispheric transport and deposition of oxidized nitrogen,  
641 *Geophys. Res. Lett.*, 35, L17815, doi:10.1029/2008GL035389, 2008.  
642
- 643 Simpson, D., Butterbach-Bahl, K., Fagerli, H., Kesik, M., Skiba, U., Tang, S. (2006). Deposition and  
644 emissions of reactive nitrogen over European forests: a modelling study. *Atmospheric Environment*  
645 40(29), 5712–5726, doi: 10.1016/j.atmosenv.2006.04.063
- 646 Solazzo et al. (2017) *Atmos. Chem. Phys.*, 17, 3001–3054 [www.atmos-chem-phys.net/17/3001/2017/](http://www.atmos-chem-phys.net/17/3001/2017/)  
647 doi:10.5194/acp-17-3001-2017  
648
- 649 Tørseth, K., Aas, W., Breivik, K., Fjæraa, A. M., Fiebig, M., Hjellbrekke, A. G., Lund Myhre,  
650 C., Solberg, S., and Yttri, K. E.. (2012): Introduction to the European Monitoring and Evaluation  
651 Programme (EMEP) and observed atmospheric composition change during 1972–2009, *Atmos. Chem.*  
652 *Physics*, 12, 5447–5481, doi:10.5194/acp-12-5447-2012, URL [http://www.atmos-chem-](http://www.atmos-chem-phys.net/12/5447/2012/)  
653 [phys.net/12/5447/2012/](http://www.atmos-chem-phys.net/12/5447/2012/), 2012  
654
- 655 Vivanco, M.G., Bessagnet, B., Cuvelier, C., Theobald, M.R., S.Tsyro, , Pirovano, G., Aulinger, A.,  
656 Bieser, J., Calori, G., Ciarelli, G., Manders, A., Mircea, M., Aksoyoglu, S., Briganti, G., Cappelletti, A.,  
657 Colette, A., Couvidat, F., D'Isidoro, M., Kranenburg, R., Meleux, F., Menut, L., Pay, M.T., Rouil, L.,  
658 Silibello, C., Thunis, P., Ung, A. (2016): Joint analysis of deposition fluxes and atmospheric  
659 concentrations of inorganic nitrogen and sulphur compounds predicted by six chemistry transport models  
660 in the frame of the EURODELTAIII project, *Atmospheric Environment* (2016),  
661 doi:10.1016/j.atmosenv.2016.11.042.  
662



663 Walker, J.T., Dombek, T.L., Green, L.A., Gartman, N., Lehmann, C.M.B. (2012). Stability of organic  
664 nitrogen in NADP wet deposition samples. Atmos. Environ. 60, 573-582, doi:  
665 10.1016/j.atmosenv.2012.06.059

666

667 Whitfield C, Strachan I, Aherne J, Dirnböck T, Dise N, Franzaring J, C.P., Hall, J., Hens, M., van  
668 Hinsberg, A., Mansat, A., Martins-Louçao, M.A., Mohaupt-Jahr, B., Nielsen, K.E., Pesch, R., Rowe, E,  
669 Santamaría, J.M. (2011): Assessing nitrogen deposition impacts on conservation status. Working group  
670 report. In: Hicks WK, et al, editors. Nitrogen deposition and Natura 2000: science and practice in  
671 determining environmental impacts. COST729/Nine/ESF/CCW/JNCC/SEIworkshop proceedings COST.  
672 p. 88–100.

673



674

675 **Table 1:** Abbreviation used in this publication

Wet deposition of oxidized N	WNO3_N
Wet deposition of reduced N	WNH4_N
Wet deposition of S	WSO4_S
Dry deposition of oxidized N	DNO3_N
Dry deposition of reduced N	DNH4_N
Dry deposition of S	DSO4_S
Atmospheric concentration of N from nitric acid	HNO3_N
Atmospheric concentration of N from nitrate in PM <sub>10</sub>	PM_NO3_N
Total oxidized N concentration = HNO <sub>3</sub> _N + PM_NO3_N	TNO3_N
Atmospheric concentration of N from ammonia	NH3_N
Atmospheric concentration of N from ammonium in PM <sub>10</sub>	PM_NH4_N
Total reduced N concentration = NH <sub>3</sub> _N + PM_NH4_N	TNH4_N
Atmospheric concentration of S	SO2_S
Atmospheric concentration of S from sulphate in PM <sub>10</sub>	PM_SO4_S
Total S concentration = SO <sub>2</sub> _S + PM_SO4_S	TSO4_S
Precipitation	PRECIP

676

677



Table 2. Meteorological and CTM model used by each participant.

	AQMEII3		EDT	
	METEO	CTM	METEO	CTM
AQ_DE1_HTAP	COSMO-CLMy	CMAQ (v4.7.1)	WRF-Common*	CHIMERE (Chimere2017b v1.0)
AQ_DK1_HTAP	WRF	DEHM	WRF-Common (adapted to different projection )	CMAQ (v5.0.2)
AQ_FI1_HTAP/_MACC	ECMWF	SILAM	WRF-Common	EMEP (rv4.7)
AQ_FRES1_HTAP	ECMWF	CHIMERE (vchim2013)	RACMO2 (nudged)	LOTOS (v1.10.005)
AQ_UK1_MACC	WRF	CMAQ (v5.0.2)	HIRLAM	MATCH (VSOA April 2016)
AQ_UK2_HTAP	WRF	CMAQ (v5.0.2)	WRF-Common	MINNI (V4.7)
AQ_TRI_MACC	WRF	CMAQ (v4.7.1)		

• Colette et al. 2017



682

683

684 **Table 3:** Number of sites for each pollutant

WNO3: 59	TNO3: 45	HNO3: 12	PM_NO3: 32
WNH4: 61	TNH4: 39	NH3: 12	PM_NH4: 27
WSO4: 61	SO2: 57	TSO4: 18	PM_SO4: 21

685

686

687 **Table 4:** The three metrics relating modelled concentrations (M) with the observed values (O), used for evaluating  
688 **model performance.**

<b>NMSE</b>	$NMSE = \frac{(O - M)^2}{O \cdot M}$	<b>&lt;= 1.5</b>
<b>FB</b>	$FB = \frac{2(\bar{M} - \bar{O})}{(\bar{O} + \bar{M})}$	<b> FB  &lt;= 0.3</b>
<b>FAC2</b>	Fraction of model estimates within a factor of two of the observed values	<b>FAC2 &gt;= 0.5</b>
	$0.5 \leq \frac{M}{O} \leq 2.0$	

689

690



Table 5. Coverage representation, mean ensemble deposition a critical load exceedance for major terrestrial habitat classes within the Natura 2000 network.

Habitat group	EUNIS code	Habitat class	Natura 2000 <sup>a</sup>	Receptors <sup>b</sup>	Avg. Dep (kg N/ha) <sup>c</sup>	CL (kg N/ha) <sup>d</sup>	CL <sub>exc</sub> <sup>e</sup>	CL <sub>exc</sub> (Dep.-SD) <sup>f</sup>	CL <sub>exc</sub> (Dep.+SD) <sup>f</sup>
Peatlands	D1	Raised and blanket bogs	1.9%	2.9%	5.98	7.50	24%	13%	37%
	D2	Valley mires, poor fens and transition mires	0.2%	0.1%	6.94	12.50	11%	7%	16%
	D3	Aapa, pulsa and polygon mires	2.1%	1.1%	1.49				
	D4	Base-rich fens and calcareous spring mires	0.1%	0.1%	9.02	21.25	1%	0%	2%
	D5	Sedge and reedbeds	0.5%	0.3%	8.05				
	D6	Inland saline and brackish marshes and reedbeds	< 0.1%	< 0.1%	11.34				
Grasslands	E1	Dry grasslands	0.5%	0.1%	5.41	15.75	0%	0%	0%
	E2	Mesic grasslands	14.1%	9.8%	9.02	20.00	2%	1%	3%
	E3	Seasonally wet and wet grasslands	1.8%	0.8%	8.83	16.25	5%	2%	10%
	E4	Alpine and subalpine grasslands	1.3%	1.3%	8.40	7.50	65%	15%	85%
	E6	Inland salt steppes	0.5%	0.1%	7.60				
	E7	Sparsely wooded grasslands	1.3%	0.4%	5.24				
				2.7%	3.9%	5.07	10.00	16%	5%
Shrublands	F2	Arctic, alpine and subalpine scrub	2.7%	3.9%	5.07	10.00	16%	5%	32%
	F3	Temperate and Mediterranean-montane scrub	3.6%	3.1%	4.25				
	F4	Temperate shrub heathland	< 0.1%	< 0.1%	4.67	15.00	0%	0%	1%
	F5	Arboreal and thermo-Mediterranean bushes	2.7%	2.4%	6.11	25.00	0%	0%	0%
	F6	Garrigue	0.6%	1.1%	6.39				
	F7	Spiny Mediterranean heaths	1.1%	1.1%	5.72				
	F8	Thermo-Atlantic xerophytic scrub	0.3%	0.0%	nd				
	F9	Riverine and fen scrubs	< 0.1%	< 0.1%	4.15				
	FB	Shrub plantations	0.8%	0.3%	7.63				
				25.1%	23.4%	8.50	15.00	4%	1%
Woodlands	G1	Broadleaved deciduous woodland	25.1%	23.4%	8.50	15.00	4%	1%	14%
	G2	Broadleaved evergreen woodland	1.2%	0.4%	6.88	15.00	0%	0%	5%
	G3	Coniferous woodland	20.7%	25.6%	7.83	10.00	34%	14%	53%
	G4	Mixed deciduous and coniferous woodland	9.4%	14.2%	8.61	10.75	32%	13%	58%
	G5	Early-stage woodland and semi-natural stands	7.6%	7.5%	6.16	7.50			

a) representation within the Natura 2000 network; b) representation within the Natura 2000 network in the joint of the buffered areas; c) weighted mean of N deposition for each habitat class according to ensemble results; d) attributed critical load in this work (based on empirical critical loads from Bobbink and Hetteling, 2011); e) area withstanding an exceedance of the CL, expressed as percentage of the total area evaluated for each particular habitat class; f) area withstanding an exceedance of the CL, when using an ensemble deposition value of mean minus/plus the standard deviation of the ensemble mean

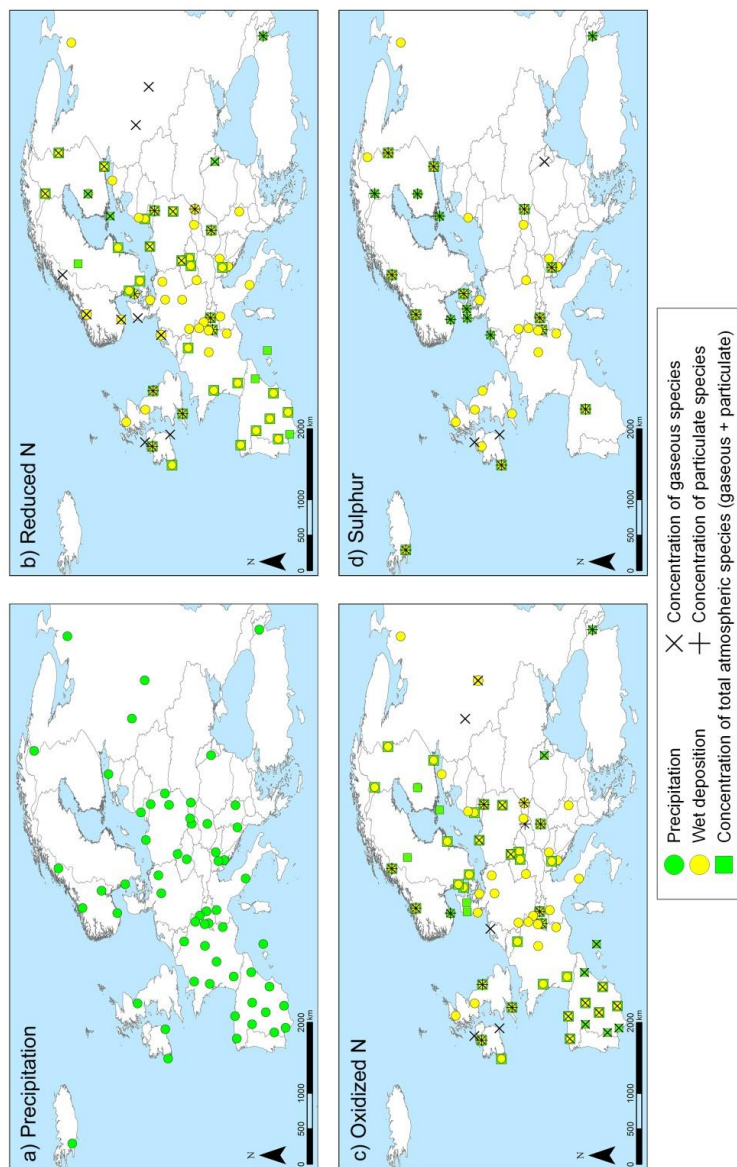
691

692

693

694

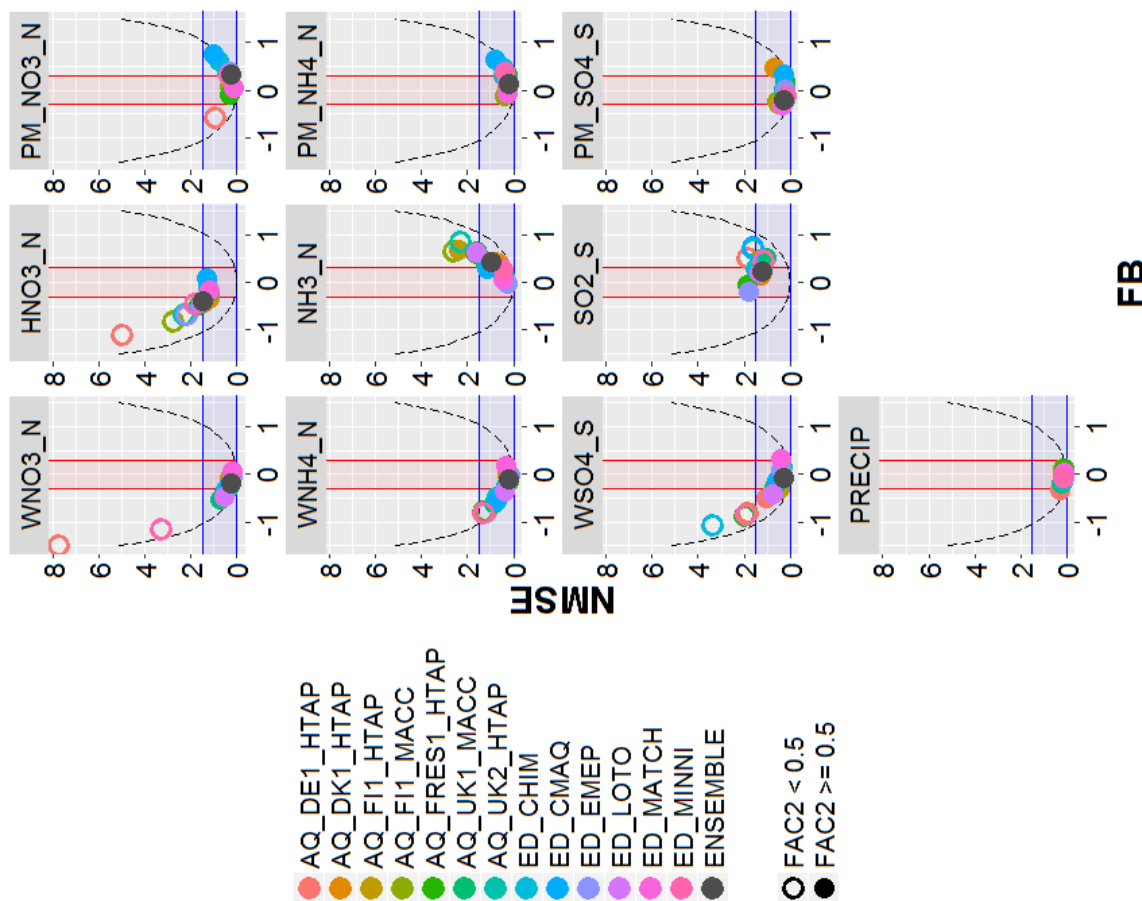
695



696

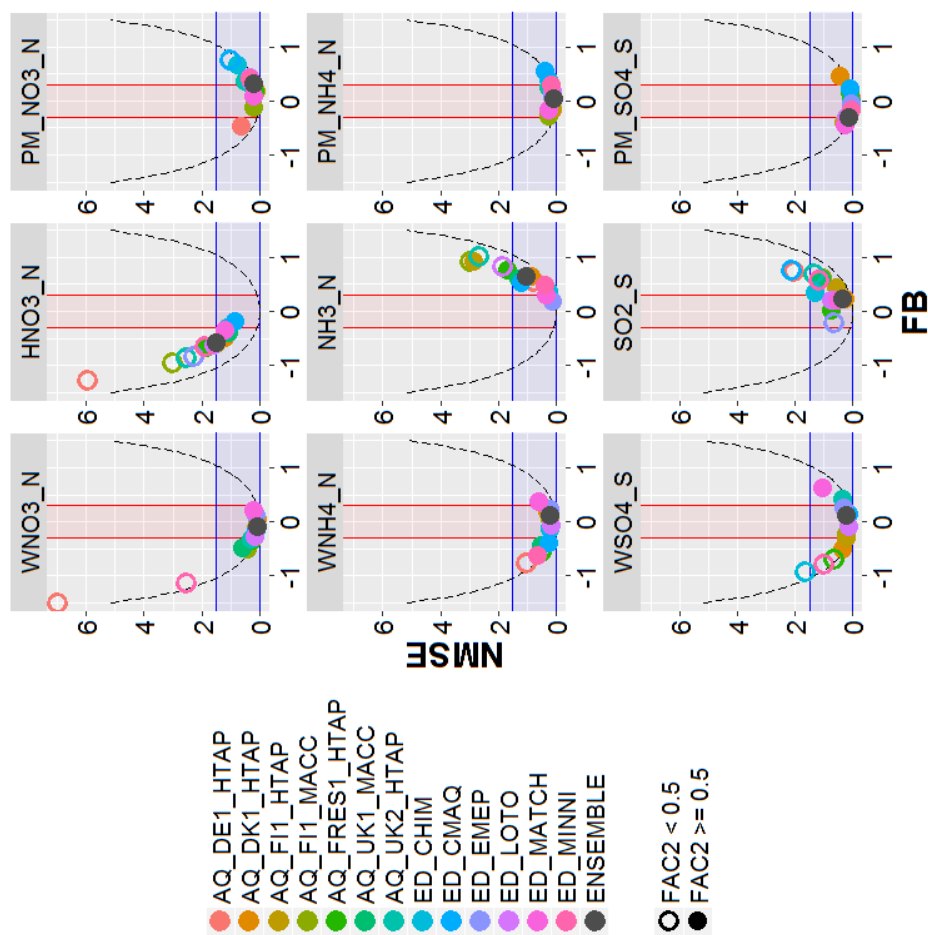
697 Figure 1: Monitoring sites with measurements of precipitation (a), reduced N species (b), oxidized N species (c) and S (d)  
698 used in the evaluation of annual modelled values.





699  
 700  
 701  
 702  
 703  
 704

Figure 2: Statistics (FB, NMSE and FAC2) calculated from annual values of wet deposition, concentration and precipitation at all available sites. Shaded areas correspond to areas meeting the acceptance criteria of Chang and Hanna (2004) (blue for NMSE, red for FB). Parabolic dashed lines indicate the theoretical minimum NMSE for a given value of FB. Better model performance is indicated by points that fall within the blue and red shaded areas and with filled circles.

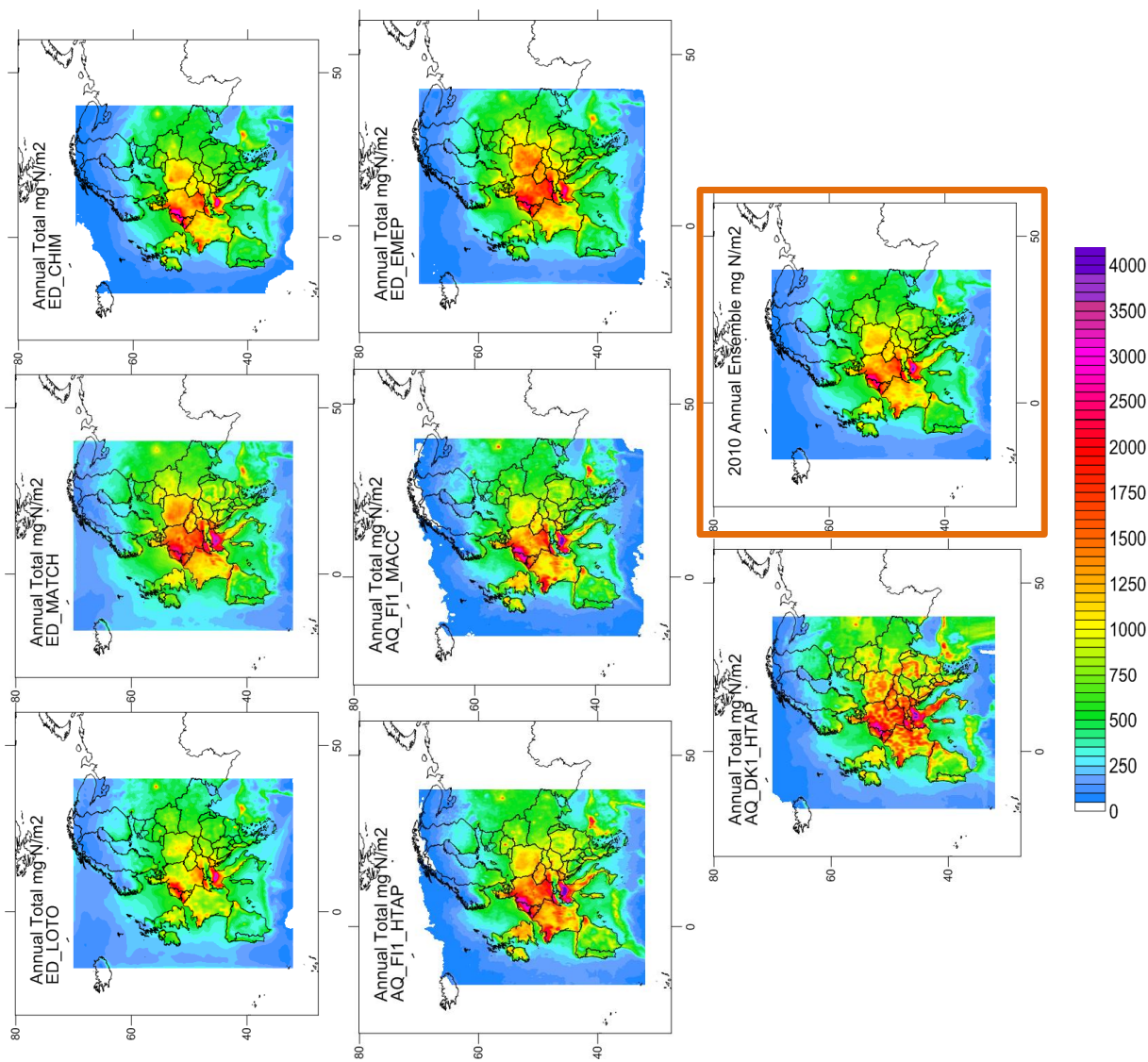


705

706  
 707 Figure 3: Statistics calculated from annual values (accumulated deposition or average means for air concentration) only at  
 708 sites with simultaneous measurements of the three related pollutants (e.g. HNO<sub>3</sub>, PM<sub>10</sub> and WNO<sub>3</sub>) for oxidised N,  
 709 reduced N and S species. Shaded areas correspond to areas meeting the acceptance criteria of Chang and Hanna (2004) (blue  
 710 for NMSE, red for FB). Parabolic dashed lines indicate the theoretical minimum NMSE for a given value of FB. Better  
 711 model performance is indicated by points that fall within the blue and red shaded areas and with filled circles.



## Annual deposition of TOTAL N



712

713

714

715

716

717 Figure 4: Maps of total N ( $\text{mg N m}^{-2}$ ) for the models showing acceptable performance for wet N deposition. The ensemble (mean of the  
718 models) is shown in right bottom panel

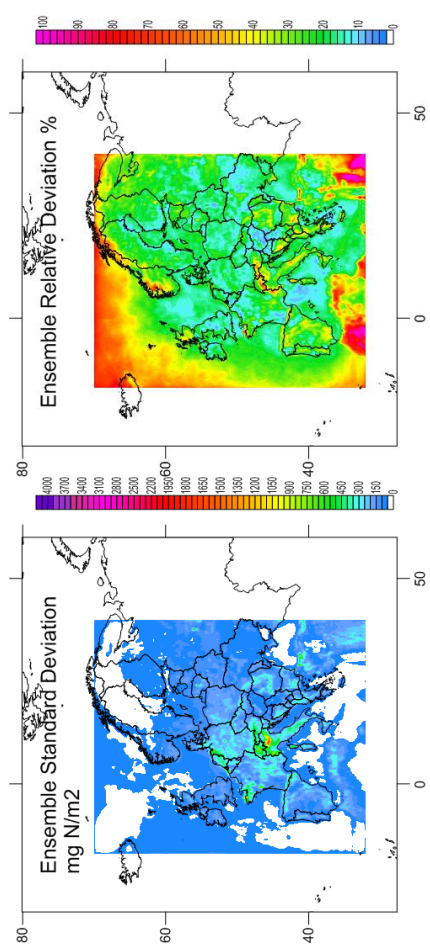


Figure 5: Maps of standard deviation of total N in absolute and relative units ( $\text{mg N m}^{-2}$ ; % of annual mean) for the ensemble.

719

720

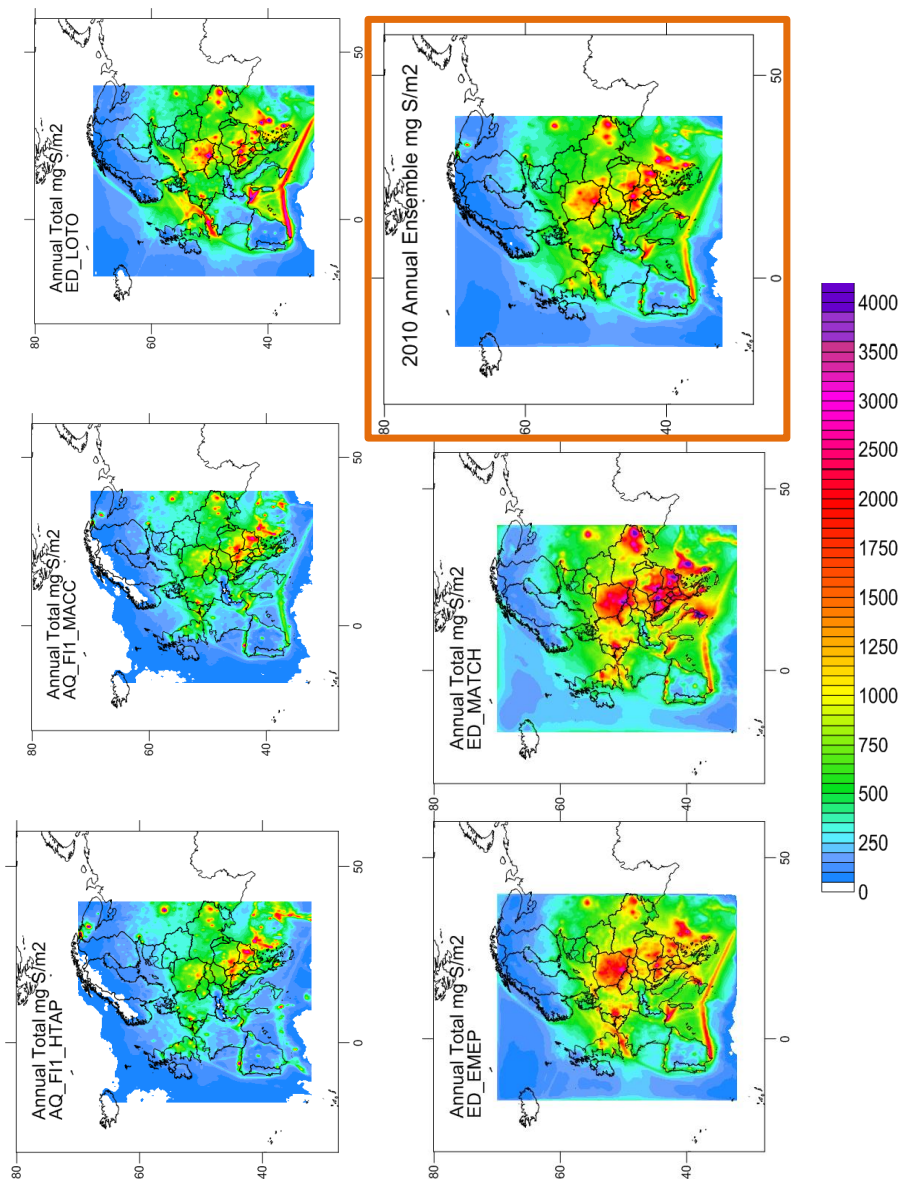
721

722

723



## Annual deposition of TOTAL S



724  
725  
726  
727  
728  
729  
Figure 6: Maps of total S ( $\text{mg N m}^{-2}$ ) for the models showing acceptable performance for wet S deposition. The ensemble (mean of the models) is included (right bottom map)

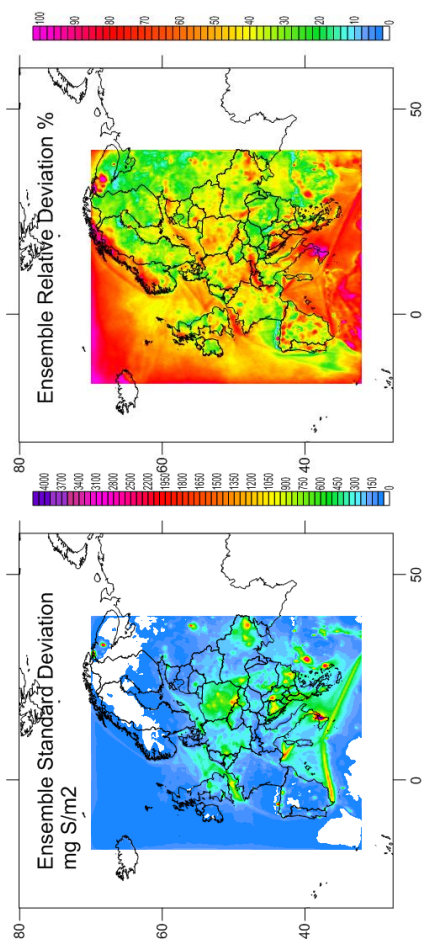


Figure 7: Maps of standard deviation of total S in absolute and relative units ( $\text{mg S m}^{-2}$ ; % of annual mean) for the ensemble.

730  
732  
733  
734

735  
736  
737  
738

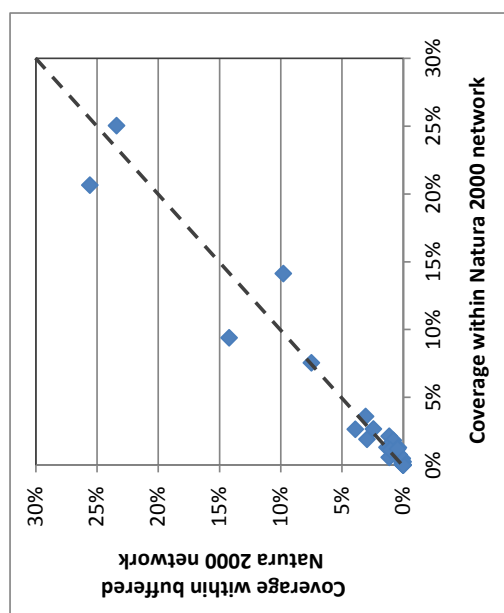


Figure 8: Coverage representation of EUNIS level-1 habitat classes within the entire Natura 2000 network versus the buffered areas.

739

740

741

742

743

744

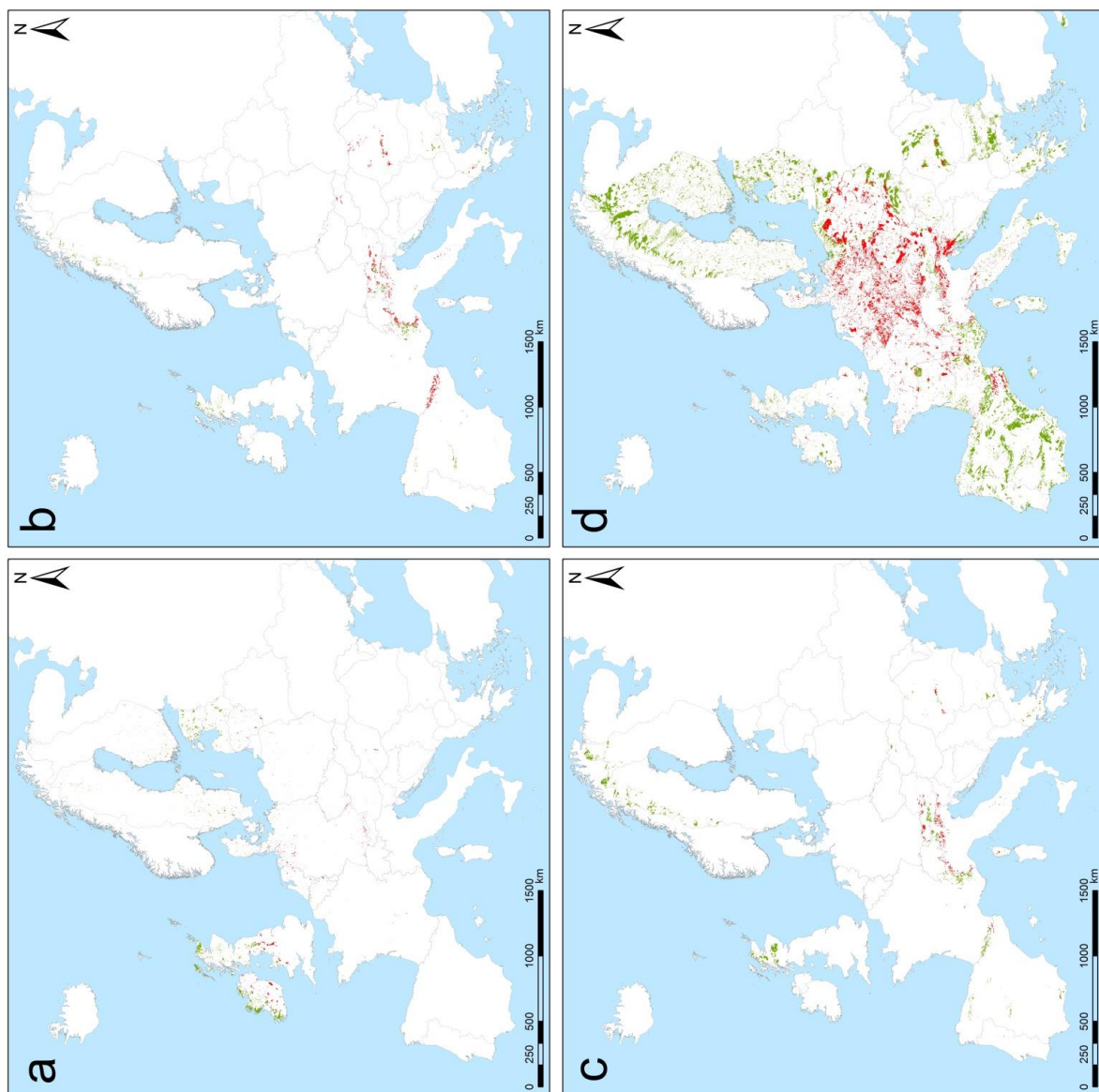


Figure 9: Habitat distribution and location of  $CL_{exc}$  for the most threatened habitat classes (a: D1 “raised and blanket bogs” and D2 “valley mires, poor fens and transition mires”; b: E4 “alpine and subalpine grasslands”; c: F2 “arctic, alpine and subalpine scrub”; d: G3 “coniferous woodlands” and G4 “mixed deciduous and coniferous woodlands”). The surface areas showing a  $CL_{exc}$  are represented in red, while the areas with no  $CL_{exc}$  are represented in green.

745  
746  
747  
748  
749  
750



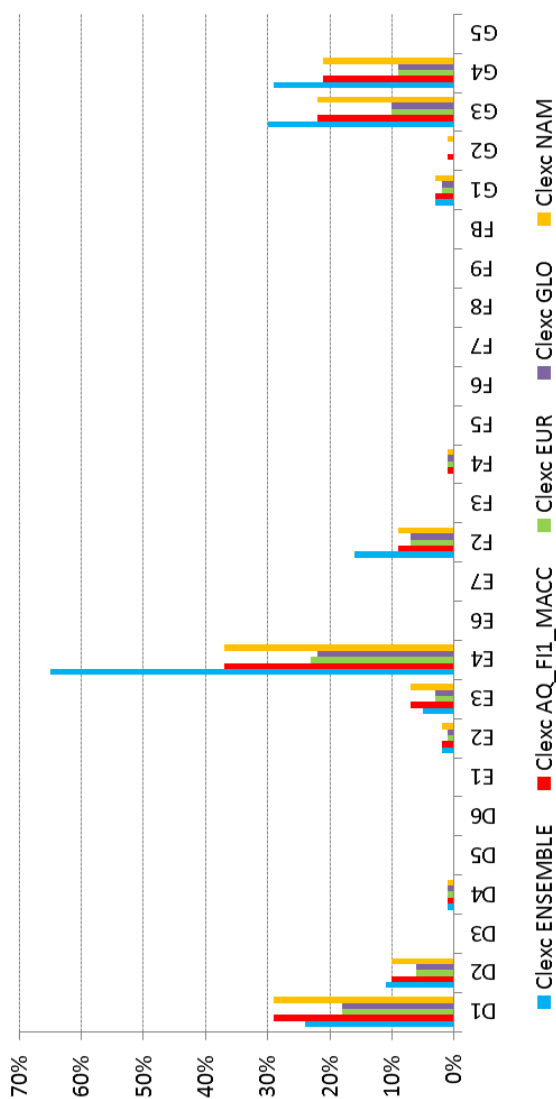
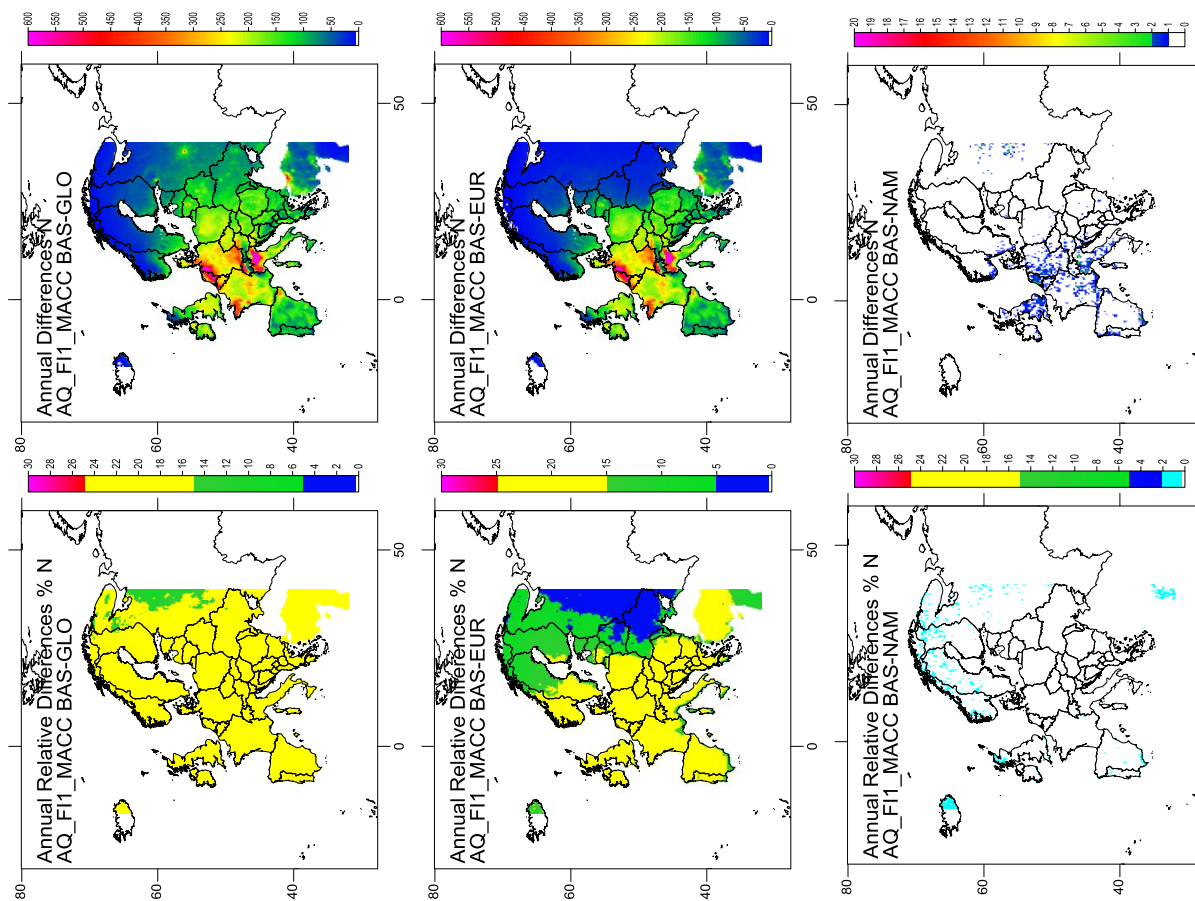


Figure 10:  
 Figure 10: Proportion of habitat area for which the critical load is exceeded for major terrestrial habitat classes within the Natura 2000 network for the base case 2010 (ensemble and AQ\_FT1\_MACC) and for the EUR, GLO and NAM cases (AQ\_FT1\_MACC)

751  
 752  
 753  
 754

755  
 756  
 757  
 758  
 759



760

761

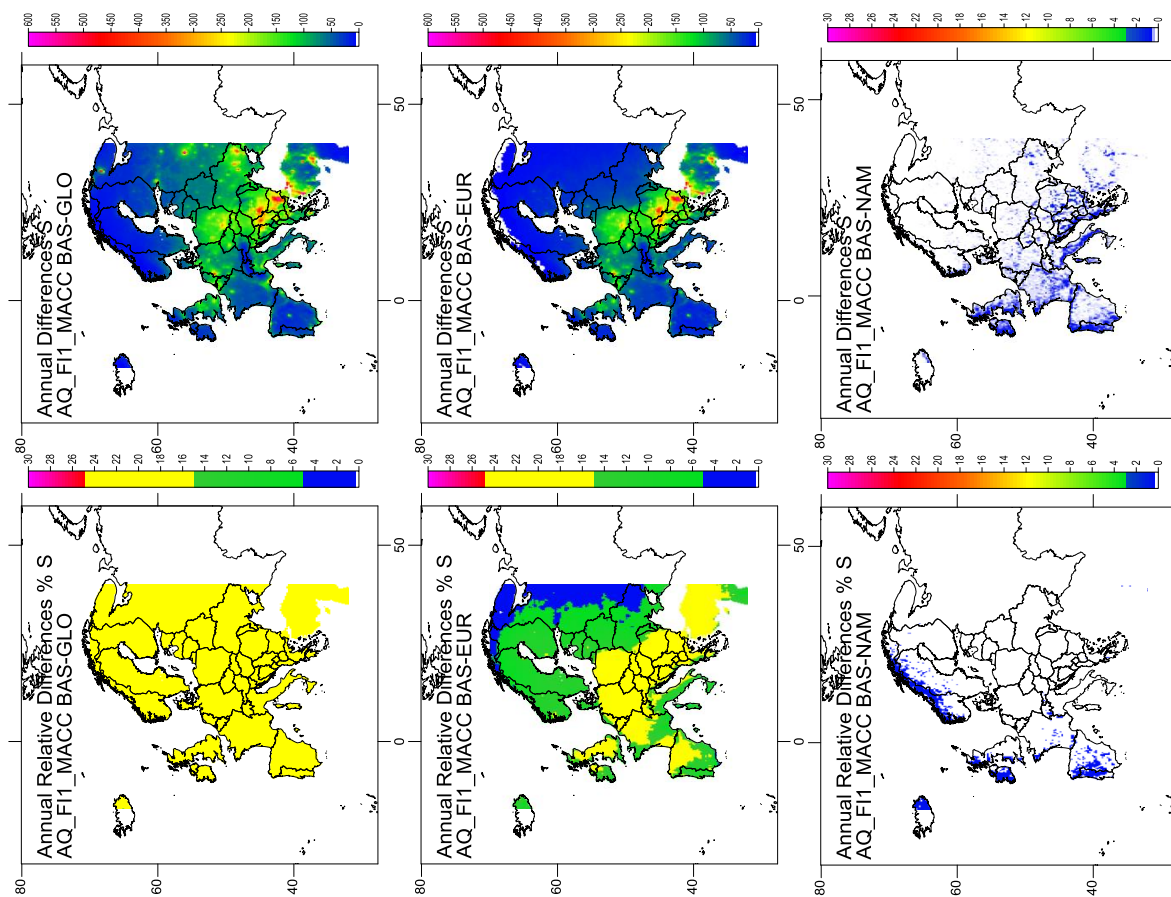
Figure 11: Effect on the N deposition in Europe of the reduction of 20% of emissions at global scale (GLO), in Europe

(EUR) and in North America (NAM), according to AQ\_FI1\_MACC (%), left, mgN/m<sup>2</sup>, right)

762

763

764



765

766

767

768

769 Figure 12: Effect on the S deposition in Europe of the reduction of 20% of emissions at global scale (GLO), in Europe (EUR)

770 and in North America (NAM), according to AQ\_FI1\_MACC (%), left, mgN/m2, right